People's Democratic Republic of Algeria
Ministry of Higher Education and Scientific Research

University M'Hamed BOUGARA – Boumerdes

Institute of Electrical and Electronic Engineering

Department of Power and Control

Final Year Project Report Presented in Partial Fulfilment of the Requirements for the Degree of

MASTER

In **Power Engineering**

Option: **Power Engineering**

Title:

Design of Sparse Matrix Converter

Presented by:

- **BOUMEDINE Youcef**
- **REZIKI Mohamed Lamine**

Supervisor:

Dr.B.METIDJI

Registration Number:……/2018

Dedication

I have the great pleasure to dedicate this modest work
To my Beloved Parents
To my Dear Brothers
To all my Friends
To all my Teachers from primary school to my last year of University.

Dedication

I have the great pleasure to dedicate this modest work
To my Beloved Parents
To my Dear Sisters
To all my Friends
To all my Teachers from primary school to my last year of University.

ACKNOWLEDGEMENT

I thank God Almighty, for giving me strength, direction, and determination.

I would like to thank the following:

I would like to express my deepest appreciation to all those who provided me the possibility to complete this project. A special gratitude I give to our final year project supervisor, Dr.Brahim METIDJI, Dr. Abdelkarim AMMAR, Mr.Hichem FACI, Mr.Walid TOUZOULT for their everlasting patience, understanding, guidance,

and support through the whole time .My parents for everlasting love, understanding, and encouragement during all times. Furthermore I would also like to acknowledge with much appreciation all my colleagues for their help and support.

Abstract

The aim of this project is to design and implement the Sparse Matrix Converter. The Sparse Matrix Converter consist of 15 Transistors, 18 Diodes, and 7 Isolated Driver Potentials. Compared to the direct matrix converter this type provides identical functionality, but with a reduced number of power switches and an improved zero DC-link current commutation scheme. It provides lower control complexity and higher safety and reliability. In the matrix converter, modulation and control techniques are so far the principal topic of research and development as the practical experience is still very limited since it is a new technology still in development. MATLAB/SIMULINK modeling and simulation of the Sparse Matrix Converter loaded by passive RL load are performed. Also, the necessary hardware has been implemented. It can be noticed that the three-phase sparse matrix converter can be used to replace of the conventional rectifier-inverter based converter. The advantages of the Sparse Matrix Converter in short are the inherent four-quadrant operation and the absence of bulky DC-link electrolyte capacitors, new control methods (SVM), and applications.

Table of Content

Table of content

Table of Content

Table of Content

List of Figures

Liste of Figures

Liste of Figures

List of Tables

Acronyms

AC	Alternating Current
B2B	Back-to-Back
CSI	Current Source Inverter
CSR	Current Source Rectifier
FPGA	Field Programmable Gate Array
IGBT	Insulated Gate Bipolar Transistor
IMC	Indirect Matrix Converter
MC	Matrix Converter
MOSFET	Metal-Oxide Semiconductor Field Effect Transistor
NCC	Naturally Commutated Cycloconverters
PWM	Pulse-Width Modulation
SV	Space Vector
SVPWM	Space Vector Pulse-Width Modulation
SMC	Sparse matrix converter.
SVM	Space Vector Modulation
THD	Total Harmonic Distortion
VHDL	Very high Development Language
VSI	Voltage Source Inverter
VSR	Voltage Source Rectifier
VSMC	Very Sparse Matrix Converter
USMC	Ultra Sparse Matrix Converter

Introduction

AC-AC converter used nowadays has an intermediate DC link with large storage capacitors. However, these last ones originate additional losses, and increase the converter weight, cost and volume. For this reason, in the last few decades an increasing interest in a new type of converters, such as Matrix converters, with nearly no storage devices, has been noticed.

These converters are capable of performing a direct AC/AC conversion, allow bidirectional power flow, guarantee input and output sinusoidal voltages and currents with variable amplitude and frequency and adjustable power factor.

Nevertheless, Matrix Converters or CMC (Conventional Matrix Converter) show some disadvantages, such as the high number of power semiconductor (18 IGBTs and 18 diodes). Therefore, with the goal of reducing the number of power semiconductors, several new topologies of AC-AC converters have been developed.

The Indirect Matrix Converter (IMC), based on the rectifier-inverter topology (without DC link storage capacitors) appeared as the first alternative to the CMC, having similar performances. Based on that topology, some researchers concluded that the indirect conversion could be equally assured even with the reduction of three IGBTs. This led to the Sparse Matrix Converter topology.

The Sparse Matrix Converter is an AC/AC converter which offers a reduction in number of components, a low-complex modulation scheme, and low realization effort. Sparse Matrix Converters avoid the multistep commutation procedure of the Conventional Matrix Converter improving system reliability and output voltage quality at the load. The sparse matrix converter topology hs 15 IGBT’s, 18 Diodes and 7 isolated driver potentials.

Compared to the Matrix Converter, this topology provides identical functionality, but with a reduced numbers of switches and improved zero dc-link current commutation scheme, which provides lower control complexity and higher safety and reliability.

The converter modulation is done at a high switching frequency using the Space Vector Modulation technique, which is based on the space vectors representation. To assure

robust control and reduced response times, sliding mode controllers have been chosen, associated to the space vectors representation.

This report contains five main chapters and a conclusion, the **first chapter** will be a short introduction to AC-AC converters, with and without DC link storage element. In this chapter the topologies, general operation and properties of several types of converters are discussed.

In **Chapter 02**, the different topologies of the Matrix Converter are investigated, with special focus given to the Sparse Matrix Converter.

Chapter 03 deals with the modulation and control methods used in the Sparse Matrix Converter, with special focus and discussion given to the space vector theory. The most powerful modulation techniques, namely the "space vector pulse width modulation (SVPWM)" is used.

In **chapter 04**, a simulation of the Sparse Matrix Converter using Matlab/Simulink is performed, various waveforms of either currents and voltages are illustrated, arrangements of the pulses are discussed to show the "zero crossing" commutation method employed in the work.

Chapter 05 with a goal to concretize the different knowledge discussed above, The Sparse Matrix Converter is realized to verify the theoretical assumptions, and check the results obtained by the simulation matches the implementation .

Finally, a general conclusion is presented and further work is proposed.

CHAPTER IV

SIMULATION AND RESULTS

CHAPTER V

IMPLEMENTATION AND RESULTS

CHAPTER III

MODULATION TECHNIQUES AND CONTROL

CHAPTER II

MATRIX CONVERTER TOPOLOGIES

CHAPTER I

TYPES OF CONVERTERS

1 Types of converters

1.1 Introduction

This report is concerned with the design and implementation of a Matrix Converter for Frequency Changing Power Supply Applications. Typically such units are used to convert 50/60Hz power available in airports to a 400Hz one for aircraft supply when they are parked in their bays [1].

Matrix Converters were first mentioned in the early 1980's by Alesina and Venturini [2]. They proposed a general model and a relative mathematical theory for high-frequency synthesis converters. They stated that the maximum input-output transformation ratio possible for the new AC-AC converter is $\sqrt{3}/2$ and also, they suggested a specific modulation and a feed-back-based control implementation of the proposed converter [3]. The AC-AC Matrix Converter is optimal in terms of minimum switch number and minimum filtering requirements. A three-phase AC-AC Matrix Converter consists basically of nine bidirectional voltage-blocking current-conducting switches. These switches are arranged in a matrix and by using this arrangement any input phase can be connected to any output phase at any time. Figure 1.2 shows such arrangement [4].

AC-AC converters can be classified into two main categories; indirect converters which utilize a DC link between the source and load and direct converters that provide direct conversion. A more detailed diagram shows how the different types of AC-AC converters are categorized:

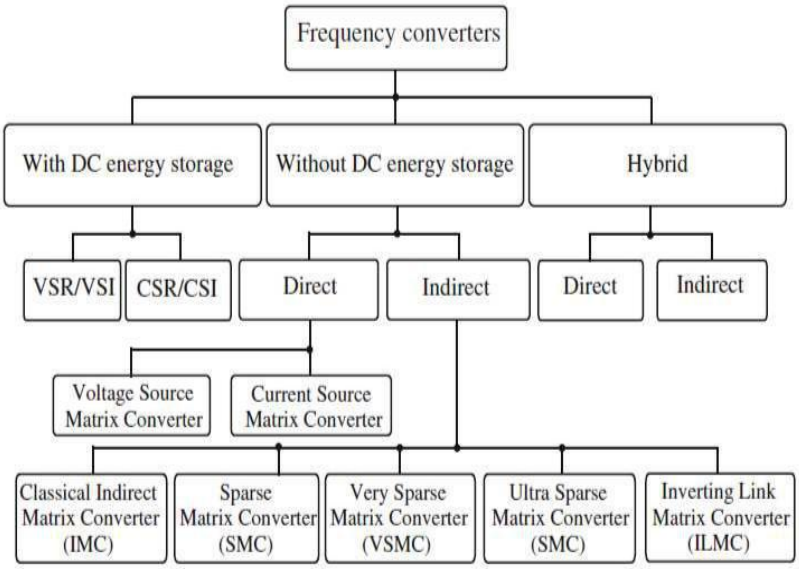

Figure 1.1: Classification of Three-Phase AC–AC Converter Topologies [26].

1.2 Indirect Converters

Indirect converters with a DC energy storage element have been investigated extensively for many years [5][6]. The DC link element of the converter can be either a capacitor for voltage source converters (VSI-VSR) or an inductor for current source converters (CSI-CSR). The indirect frequency converter with a DC energy storage element and pulse width modulation (PWM) was first reported in the mid-1970s [7] [8].

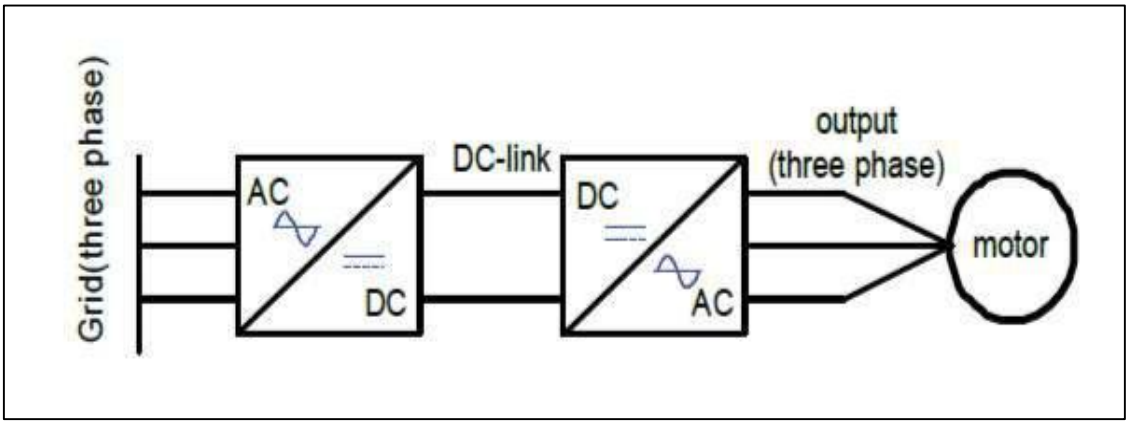

Figure 1.2: Conventional Inverter Based on AC-DC-AC Converter Block Diagram [32].

The most traditional AC–AC power converter topology is a pulse width modulated (PWM) voltage source inverter (PWM-VSI) with a front-end diode rectifier and a DC link capacitor, as shown in (Figure1.4).

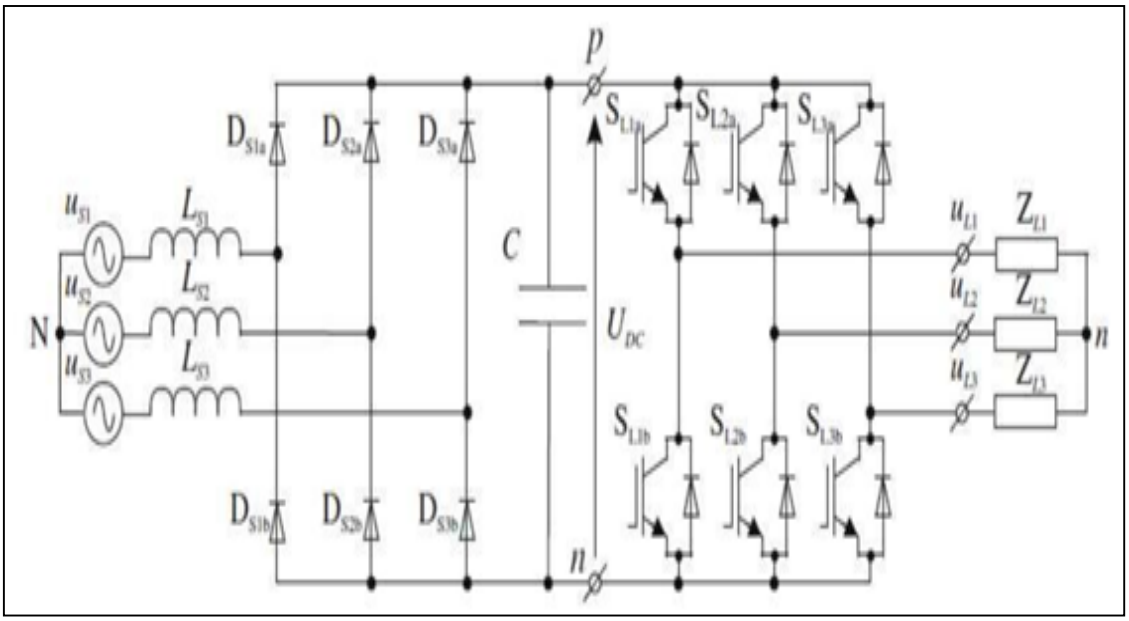

Figure1.3: Two-Level Indirect Frequency Converter with Voltage Source Inverter [26].

1 Types of converters

This type of converters is a called a “two stage converter “because it convert input AC into DC and then reconvert DC back into output AC with variable amplitude and frequency. The DC-link capacitor decouples two AC power conversion stages and ensures the independent control of two stages. The control of the output is achieved by modulating the duty cycles of the devices in the inverter stage so as to produce near-sinusoidal output currents in the inductive load, at a desired amplitude and frequency.

As the current direction in a diode rectifier cannot reverse, the lack of bidirectional power flow arises. A solution to the problem can be found by using IGBT bridge as a supply rectifier, this converter is called back-to-back inverter (B2B VSI) and is presented in Figure 1.5.

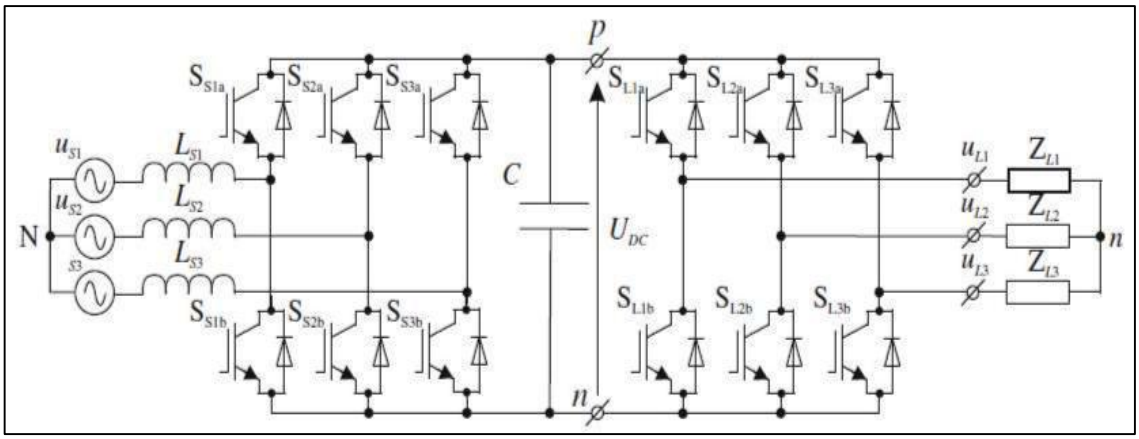

Figure 1.4: Back-to-Back Converter (BB-VSI) [26].

The back-to-back converter consists simply of a force-commutated rectifier and a force-commutated inverter connected by a common DC-link, making their separate control possible.

The DC energy storage in the presented indirect frequency converters is a bulky component. In the solution with VSI, the DC link capacitors are relatively large compared to the size of the rectifier and inverter semiconductor components, at the same time reducing the speed of response. Electrolytic capacitors typically occupy from 30 to 50% of the total volume of the converter for power levels greater than a few kW and in addition to this, they are components with a limited lifetime. It should be noted that the electrolytic capacitor has by far the shortest lifetime of any element, active or passive, used in power electronic converters. In addition, the presence of the capacitor significantly limits the power converter to high temperature applications up to 300 ◦C, because these capacitors are temperature sensitive [9]. Furthermore, high power

conventional capacitors cannot be used in some special applications, such as in aeronautics, aircraft and deep-sea or space systems.

1.3 Direct Converters

Direct converters are converters having the advantage of not having the bulky DC link contained in indirect ones. After the introduction of controlled converters in 1930, it was realized that this provided the possibility of generating alternating currents of variable frequency directly from a fixed frequency AC supply the positive rectifier supplying the positive half cycles of current and the negative rectifier supplying to the negative half cycles.

This system was called cycloconverter at its early stage and this proved to be so appropriate that nowadays it is still used in some high power applications [10].

For a three-phase to three-phase cycloconverter, 36 thyristors are required. This makes that cycloconverter systems large and complicated and tend to be used in applications where high power is required (1MW and up) [11].

Today, high power, multi-megawatts, thyristor based cycloconverters are very popular for driving induction and wound field synchronous motors. Some general applications of cycloconverters are Cement and ballmill drives, rolling milldrives, and variable-speed, constant-frequency (VSCF) power generation for air-craft 400Hz power supplies [12].

A cycloconverter is an arrangement of two converter connected back to back as shown in Figure 1.6.

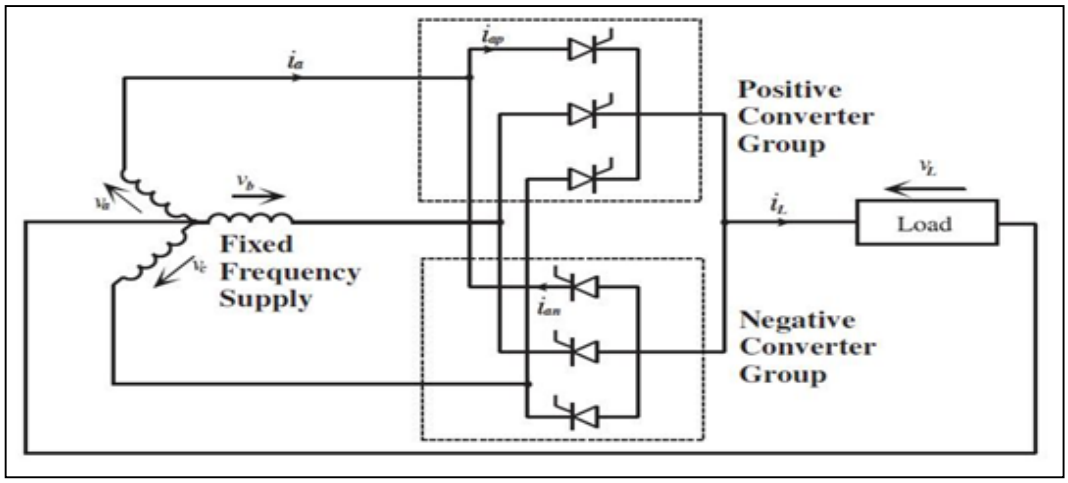

Figure 1.5: Single-Phase Load Fed From a Three-Pulse Cycloconverter [10].

1.4 Matrix Converters

One of the powerful developments of the cycloconverter is the “Matrix Converter”. Generally, the matrix converter is a single-stage converter which has an array of M x N bi-directional power switches to connect directly an m-phase voltage source to an N-phase load which is presented in Figure 1.6.

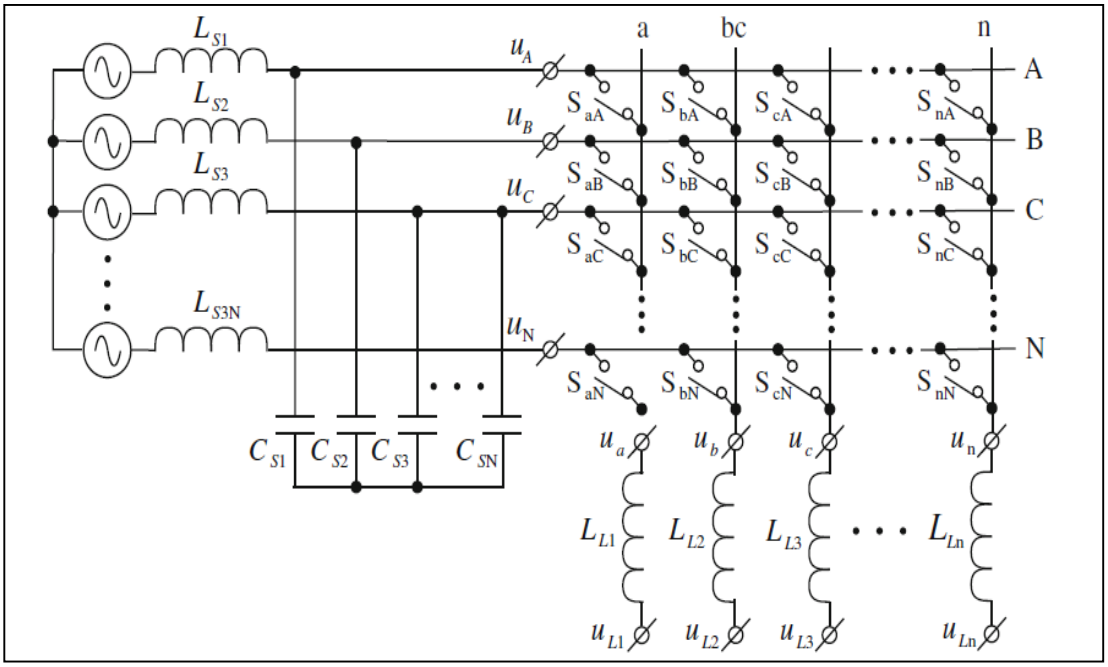

Figure 1.6 : Simplified Circuit of M× N Phase Matrix Converter [26].

In three-phase systems, an MC is an array of nine bi-directional voltage-blocking current-conducting switches that allow any load phase to be connected to any source phase.

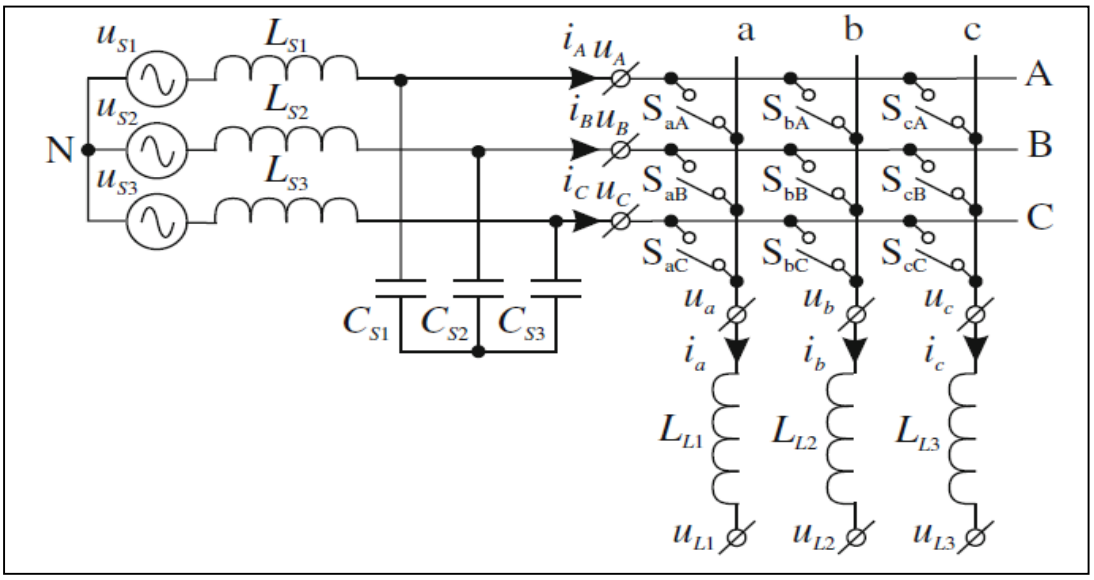

Figure 1.7: Simplified Circuit of Three-Phase Matrix Converter [26].

1 Types of converters

Matrix Converters were first mentioned in the early 1980's by Alesina and Venturini [13]. They proposed a general model and a relative mathematical theory for high-frequency synthesis converters. They stated that the maximum input-output transformation ratio possible for the new AC-AC converter is ξ and also, they suggested a specific modulation and a feed-back-based control implementation of the proposed converter [14]. The AC-AC Matrix Converter is optimal in terms of minimum switch number and minimum filtering requirements [10].

1.5 Conclusion

In this chapter, a short introduction to AC-AC converters was introduced, including both direct and indirect types, state the art of the different types of converters has been mentioned, and distinct topologies, general operation and properties also have been discussed.

2 Matrix converter topologies

2.1 Introduction

The Matrix Converter (MC) is a forced commutated converter which uses an array of controlled bidirectional switches as the main power elements to create a variable output voltage system with unrestricted frequency. It does not have any DC-link circuit and does not need any large energy storage elements [15].

The matrix converter has several advantages that make it a strong candidate for taking the lead over conventional converters in the industry, we can mention mainly 5 basics are:

1. Sinusoidal input and output voltages or currents,
2. Generation of load voltage with variable amplitude and frequency,
3. Simple and compact power circuit,
4. Operation with unity power factor, and
5. Energy regeneration capability.

These highly attractive characteristics are the reasons of the tremendous interest in this topology. The Matrix converter theory have made a bid advance when Venturini and Alesia presented their work in 1980 [16].They presented the power circuit of the converter as a matrix of bi-directional power switches and they introduced the name "Matrix Converter." One of their main contributions is the development of a rigorous mathematical analysis to describe the low-frequency behavior of the converter, introducing the "low frequency modulation matrix" concept [15]. Since then, MC's have been subject of intensive research which mostly concentrated on two aspects: implementation of the MC switches and the MC control [17].

2.2 Bi-directional Switch Construction (Configuration)

The three-phase MC topology is constructed using nine bi-directional four-quadrant switches arranged in a matrix. There are four main topologies for bi-directional switches, are shown below

2.2.1 Diode Bridge Topology

The diode bridge arrangement is the most simple bi-directional switch structure. This arrangement consists of an IGBT at the center of a single phase diode bridge arrangement, as illustrated in Figure 2.1. The main advantage of this arrangement is that only one active device is need, reducing the cost of the power circuit and the complexity of the control/gate drive circuits.

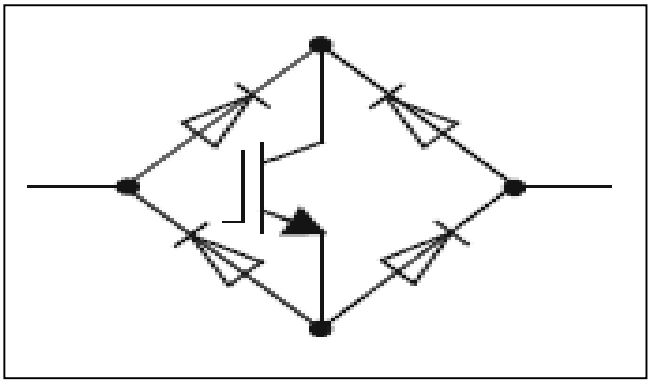

Figure.2.1: Diode Bridge Bi-directional Switch[10].

2.2.2 Common Emitter Bi-directional Switch

This switch arrangement consists of two diodes and two IGBTs connected in anti-parallel as shown in Figure 2.2.The diodes are included to provide the reverse blocking capability. The reverse blocking capability is a weak of the early IGBT technology [18] [19]. There are several advantages in using this arrangement when compared to the diode bridge switch. The first advantage is that it is possible to independency control the direction of the current.

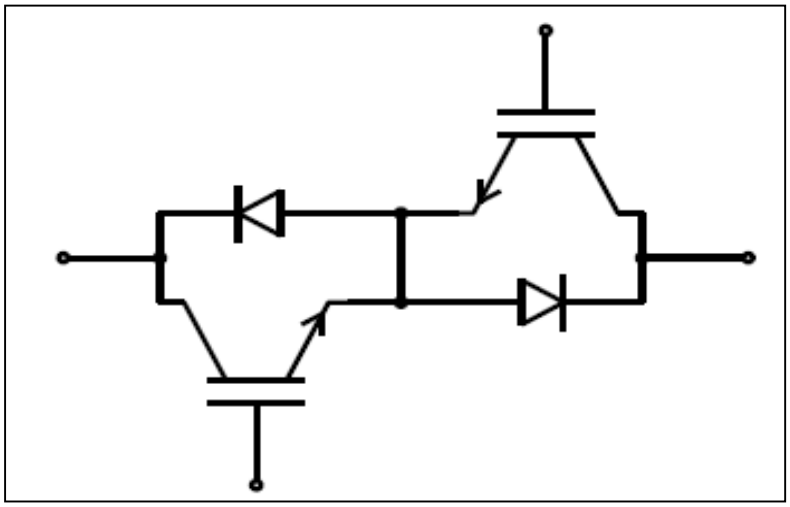

Figure 2.2: Common Emitter Bi-directional Switch [10].

2.2.3 Common Collector Bi-directional Switch

This arrangement is similar to the arrangement presented in the previous configuration. The difference is that the IGBTs are arranged in a common collector configuration as shown in Figure 2.3. The conduction losses are the same as the common emitter configuration. One possible advantage of the common collector configuration is that only six isolated power supplies are required to supply the gate drive signals.

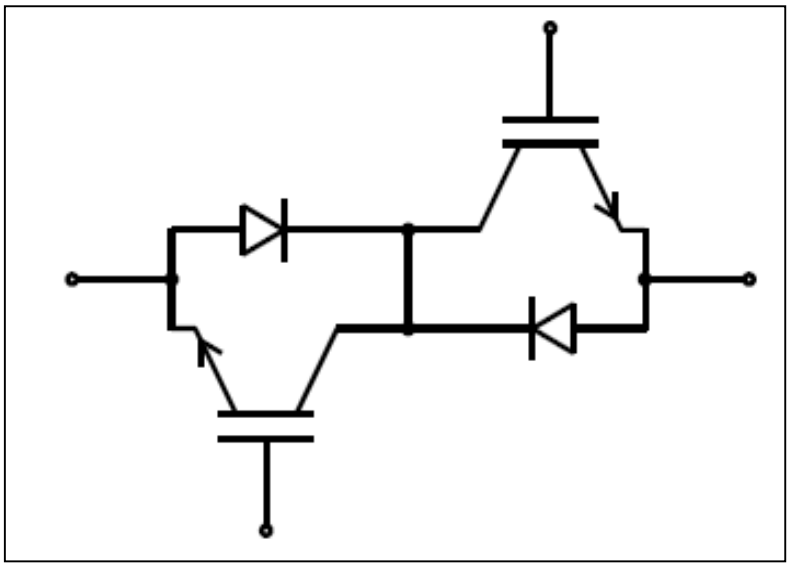

Figure 2.3: Common Collector Bi-directional Switch [10].

2.3 Matrix Converter Topology

2.3.1 Direct Matrix Converter Topology

The direct matrix converter topology consists of n x N bi-directional switches connecting the n-input line to the N-output line in order to provide a direct power conversion, [9]. The converter is characterized by its ability to connect any input phase to any output phase at any instant. An n-line input phase and N-line output phase direct matrix converter topology is shown in Figures 2-4 and 2-5.

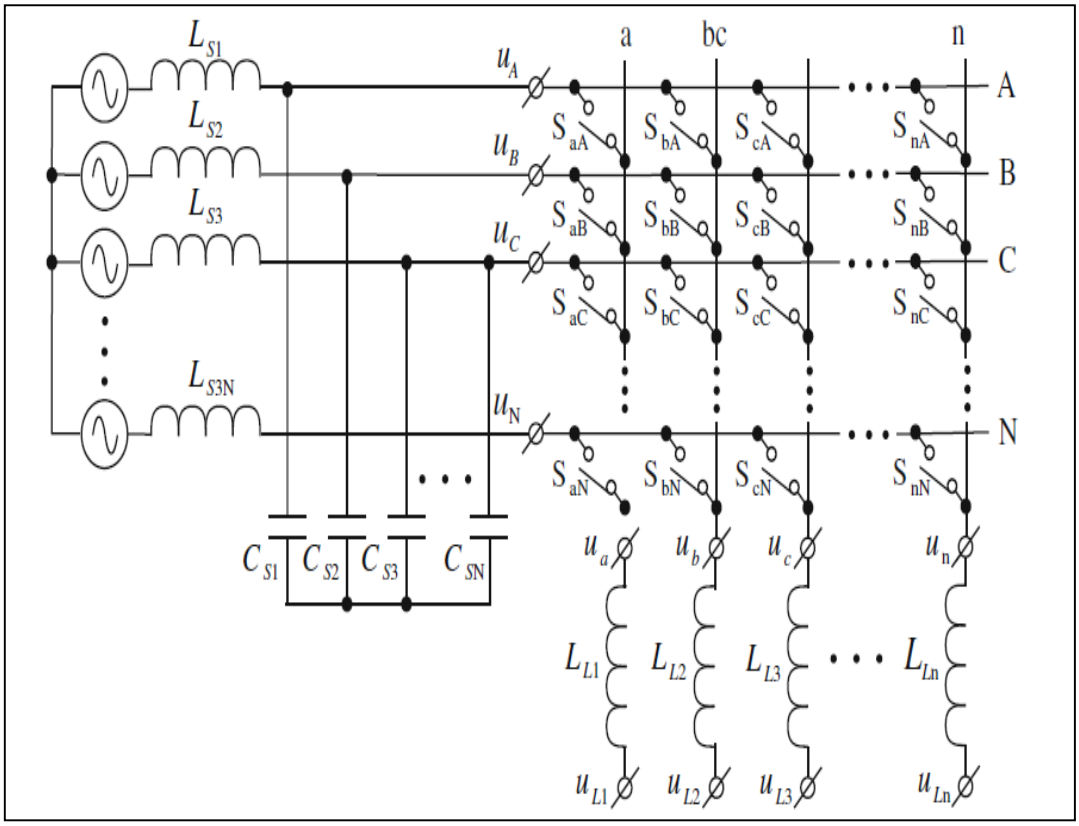

Figure 2.4: Simplified Circuit of m × n Phase Matrix Converter [26].

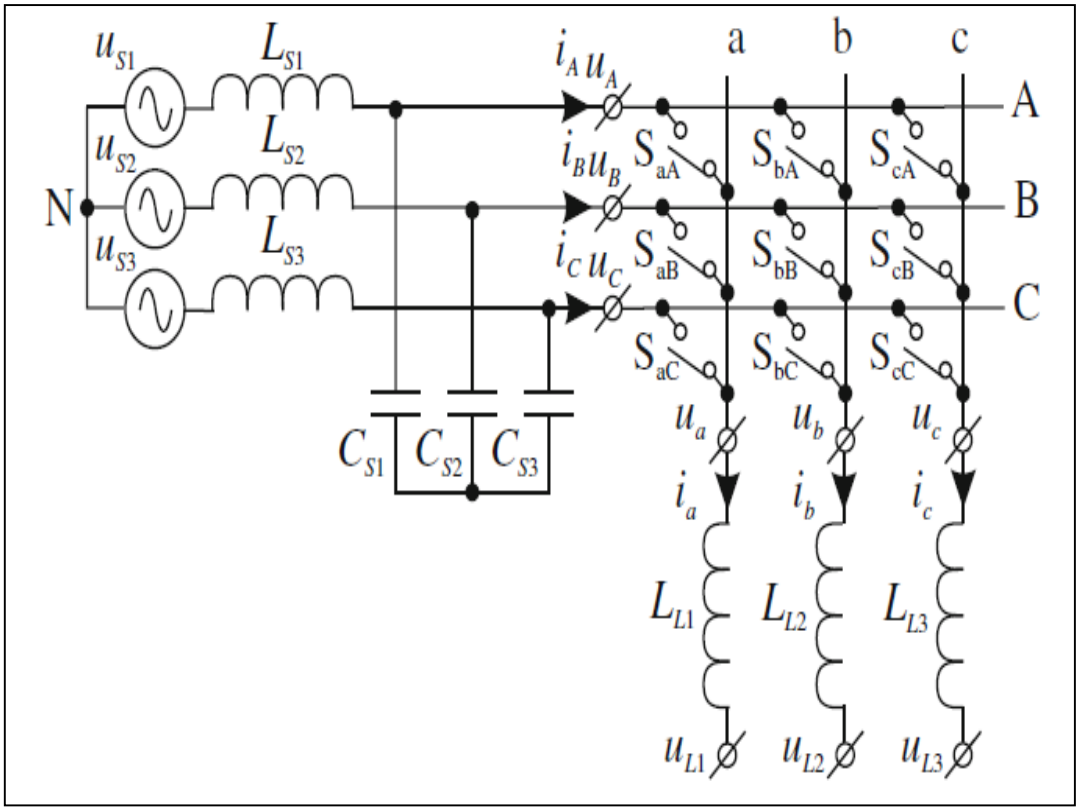

Figure 2.5: Simplified Circuit of Three-Phase Matrix Converter [26].

2.3.2 Indirect Matrix Converter Topology

It is a two -stage converter topology known as an indirect matrix converter (IMC). This topology is similar to the conventional inverter-based converter topology without any reactive DC-link energy storage components for the intermediate imaginary DC-link bus. A block diagram of the IMC topology is shown in Figure 2-6.

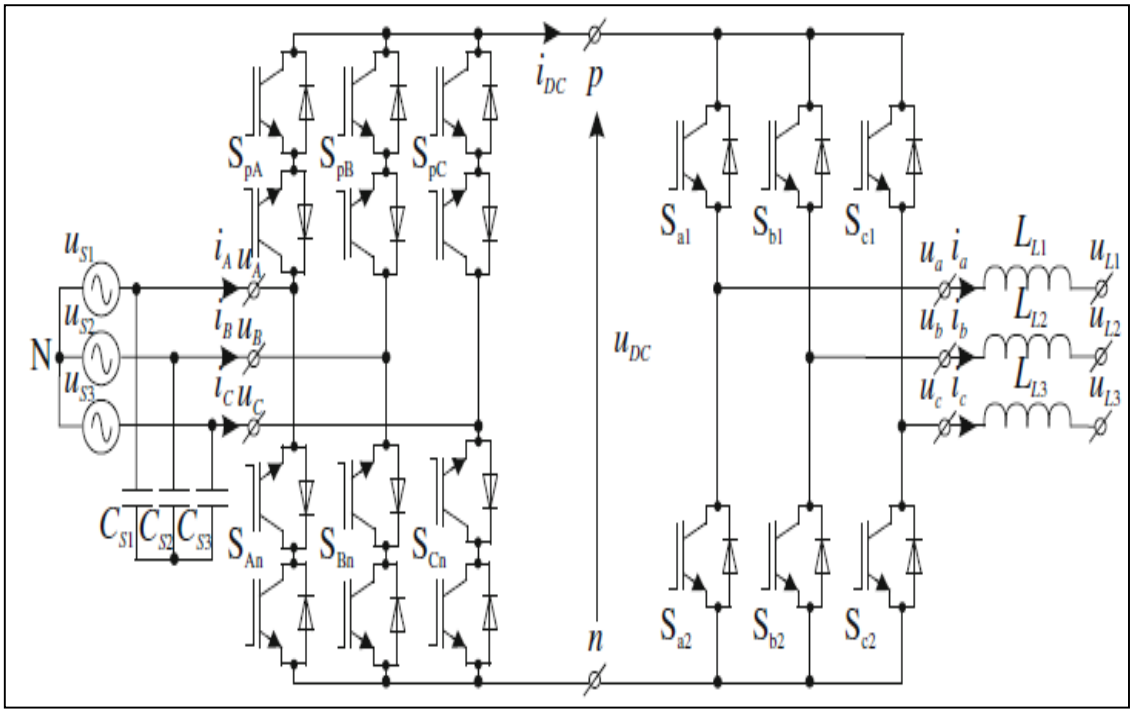

Figure 2.6: Indirect Matrix Converter [26].

All the desired features of the DMC are achieved by this IMC topology. In addition, this topology simplifies the complexity of the conventional PWM control strategy, and overcome the commutation problems of the previous topology. Besides, commutation at zero input current is possible. The IMC topology shown in Figure 2-6 is treated as a two-stage transformation converter:

- Rectifier stage to provide an imaginary DC-link during the switching cycle,
- Inverter stage to generate the three phase desired output voltages.

2.3.3 Sparse Matrix Converter Topology

This topology was developed based on the structure of the IMC topology [10], [20]. Since the topology employs a reduced number of switches compared to the CMC or IMC topologies, it is denoted as a sparse matrix converter (SMC) topology [8-9]. All the important characteristics of the indirect matrix converter topology are possibly

provided by this topology. Furthermore, the SMC topology can be reduced to a lower number of switches, and is called as the ultra sparse matrix converter (USMC) topology [8-9].

2.3.4 Derivation of Sparse Matrix Converter

The rectifier stage circuit of the IMC topology has a fixed DC-link polarity. However, the switches can operate with both DC-link polarities. Therefore, the number of switches can be reduced to 15 from 18 switches of the rectifier stage circuit of the IMC topology as shown in Figure 2-7.

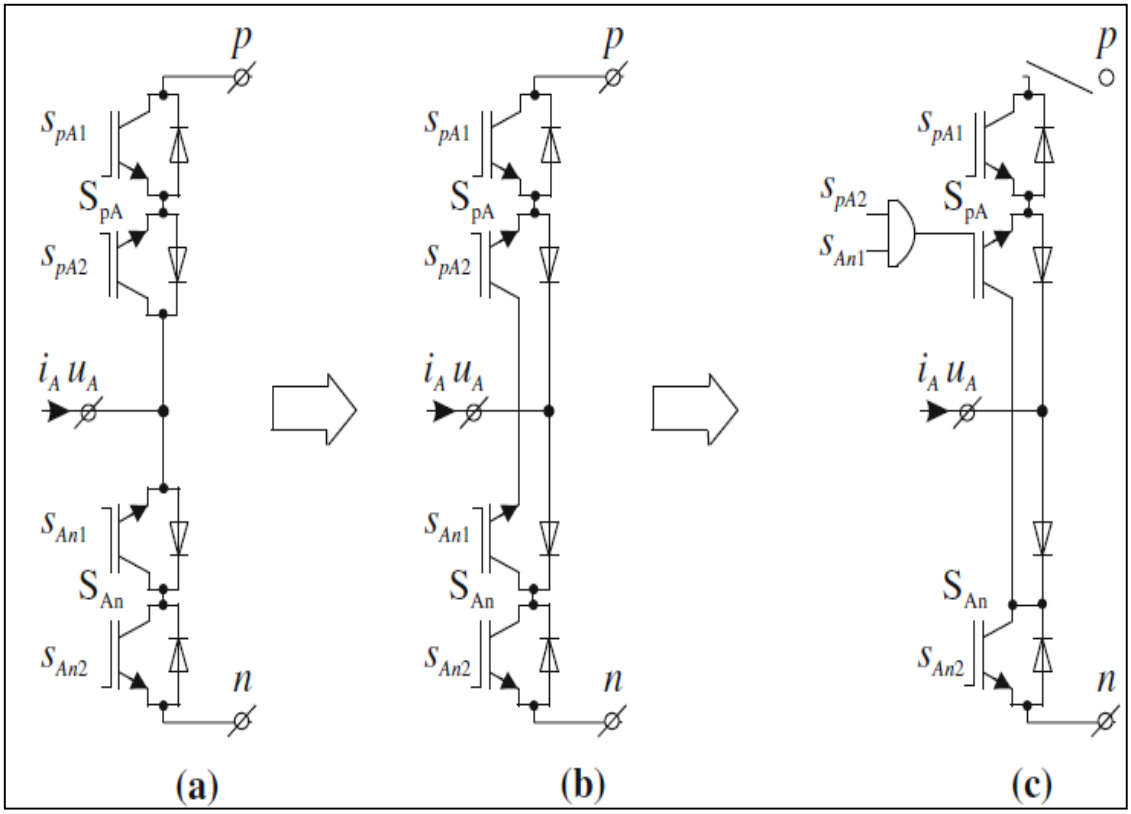

Figure 2.7: Derivation of The Bridge Branch a) Branch for IMC, b) Idea of Reduction of Branch Transistors, c) Branch for SMC [26].

The inverter stage of the SMC is the same as the indirect matrix converter topology. The same method of modulation technique, which is used by the IMC topology, can be applied to the three-phase SMC topology. A three-phase SMC topology is shown in Figure 2-8.

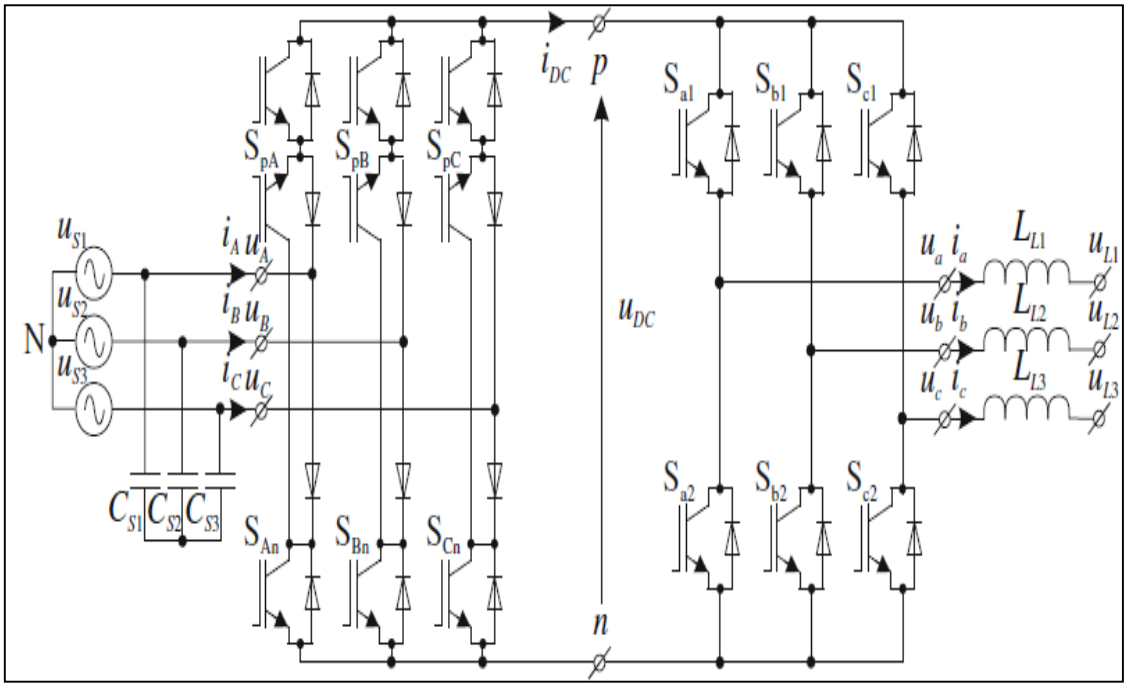

Figure 2.8: Sparse Matrix Converter Topology (SMC) [26].

2.3.5 Ultra Sparse Matrix Converter Topology

Further reduction of the switches of the sparse matrix converter (SMC) topology to 9switches is possible. The reduced topology is termed as the ultra sparse matrix converter (USMC) topology [9] as shown in Figure 2-9. There will only be a unidirectional power flow (V_{pn} >0, I_{pn} >0) , since the reduction of the topology is basedon unidirectional power flow. The ability to control the power factor of the input voltageand input current is limited to ±π/6. Besides, the maximum allowed output displacement factor is limited to ±π/6. The sparse matrix converter (SMC) modulation technique used can be extended to control the ultra sparse matrix converter (USMC) topology.

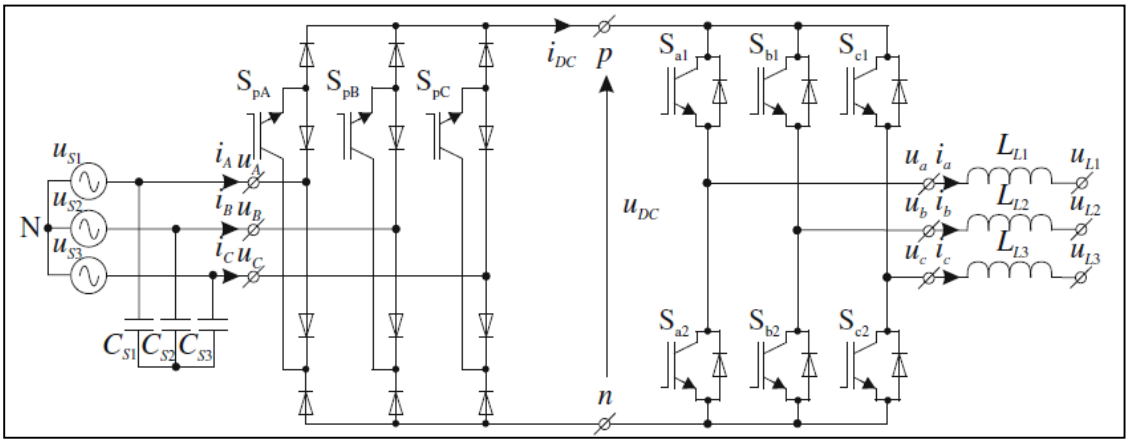

Figure 2.9: Ultra Sparse Matrix Converter Topology [26].

Alternative sparse matrix converter topologies are also proposed [9]. These are:

- Very sparse matrix converter topology
- Inverting link matrix converter topology

2.4 Commutation scheme

2.4.1 Multistep-commutation

For a given switching state of the rectifier input stage the commutation of the inverter output stage has to be performed identical to the commutation of a conventional voltage DC link converter where a dead time between turn-off and turn-on of the power transistors of a bridge leg has to be considered in order to avoid a short circuit of the DC link voltage.

For the changing of the switching state of the SMC rectifier input stage for given inverter switching state one has to ensure that no bidirectional connection between two input lines, i.e. not short circuiting of an input line-to-line voltage does occur. There, multistep commutation as known for the CMC can be employed as shown in Figure 2-10.

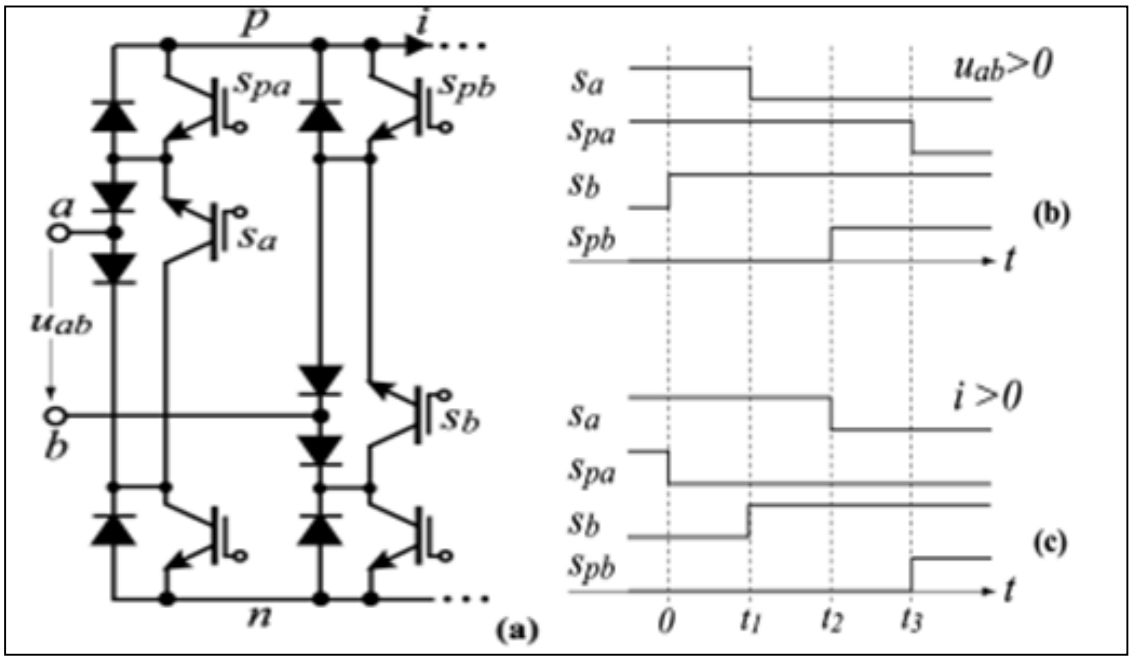

Figure 2.10: Application of Multistep Commutation to the SMC Rectifier Input Stage; (a): Basic Structure of the Commutating Bridge Legs; Switching State Sequence Given for Changing the Connection of the Positive DC Link Voltage Bus p from Input a to Input b, (b):Voltage Independent Commutation Assuming a Positive DC Link Current, i.e. i> 0,(c): Current Independent Commutation Assuming $u_{ab} > 0$[33].

2.4.2 Zero DC link current commutation

The obvious drawback of multistep commutation is limitation problem. However, AC-DC-AC (two stage) matrix converters do provide a degree of freedom for control which is not available for the CMC and can be utilized for alleviating the commutation problem. As proposed in [21], in advance to rectifier stage commutation the inverter stage could be switched into free-wheeling operation and the rectifier stage then could commutate at zero DC link current flow during commutation has to be considered and the switching losses of the input stage are reduced. One only has to ensure the no overlapping of turn-on intervals of power transistors in a half bridge occurs which would result in a short circuit of an input line-to-line voltage as shown in Figure 2-11. All further considerations in this report will be restricted to this straightforward and potentially more reliable commutation concept.

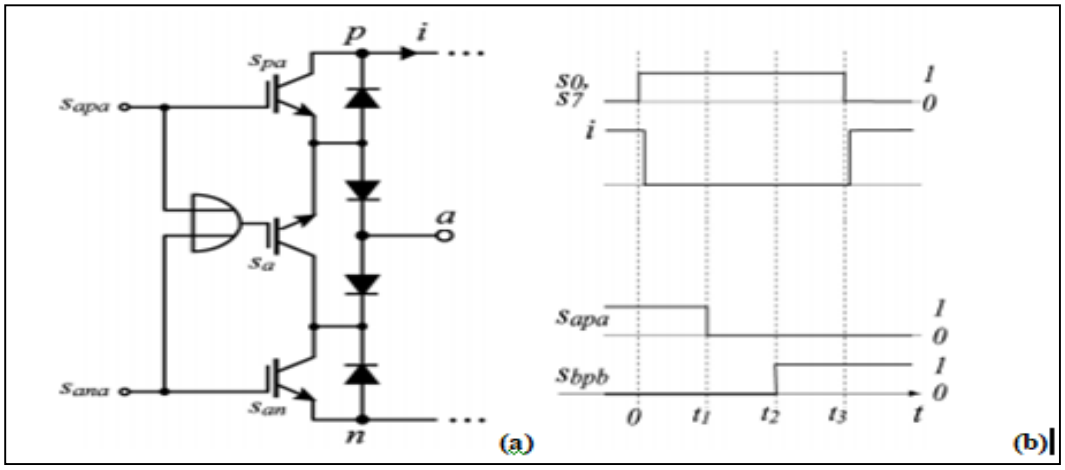

Figure 2.11: Zero Current Commutation of Indirect Matrix Converter Topologies Shown for the SMC. (a): Control of the Power Transistors of the Bridge Leg of the SMC. (b): Switching State Sequence [33].

2.5 The Clamp Circuit

The first protection scheme proposed in [13] [22] is a clamp circuit made up of one or two capacitors connected to all input and all output lines through two diodes bridges as shown in Figure 2-12.This clamp circuit is operative for all nine bi-directional switches.

It protects the switches from the surge coming from the input AC line as well as from the surge on the output side that would be otherwise produced whenever an emergency shut-down of the converter is required.

As a matter of fact, in the latter case, when the inductive currents of the motor are interrupted, the energy stored in the load is transferred to the clamp capacitor and no critical overvoltage is caused if the capacitor is large enough. Furthermore, the clamp circuit prevents output voltage spikes caused during switches commutation by the parasitic inductance of the power switch matrix and by the unavoidable timing inaccuracies.

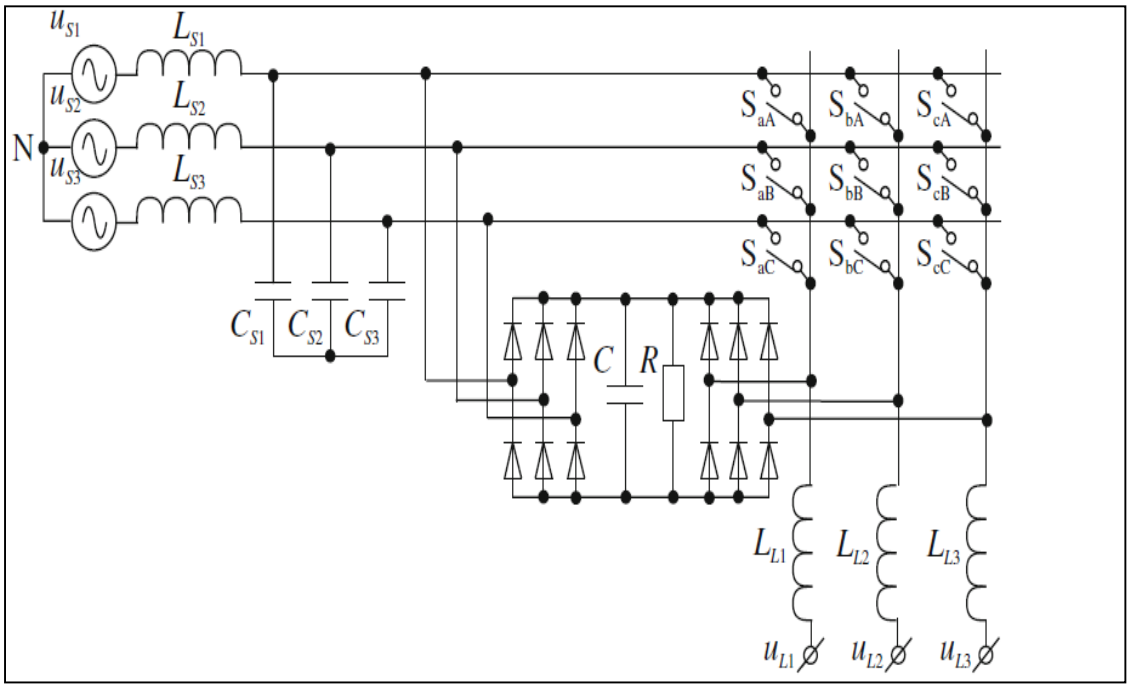

Figure 2.12: Matrix Converter with a 12-Diode Protected Clamp Circuit [26].

2.6 Conclusion

This chapter presents the background of the various different topologies of the matrix converter and a brief description of the conventional standard AC-DC-AC inverter based converter topology. Furthermore, it briefly touched on the construction of the basic building blocks of the converter (bidirectional switch). The derivation of the remaining topologies from the direct matrix converter was shown. The subsequent subsections presented the reduction of the indirect matrix converter into the sparse and ultra spares matrix converter [9].

3 Modulation techniques and control

3.1 Introduction

AC to AC power conversion can be realized by using a rectifier stage and an inverter stage or by using a Direct or Matrix Converter (MC). A Matrix Converter uses only one conversion stage compared to two stages for the rectifier /inverter solution. Each converter topology has particular advantages and disadvantages, the choice, therefore, depends on the requirements of the application. The state of the art in Matrix Converter technology is presented in this chapter. The Matrix Converter concept is introduced with the mathematical model circuit operation and associated modulation techniques. Modulation techniques used in Matrix Converters have been considered by researches for many years [7]. This report proposes different modulation techniques. The modulation techniques section of this chapter presents the main modulation techniques used in Matrix Converters. The two Venturini modulation methods [23] and the scalar modulation scheme [24] are reviewed. A detailed analysis of Space Vector Modulation (SVM) algorithms for Matrix Converters is then presented. The Matrix Converter control strategies were first mentioned by Alesina and Venturini [25]. The block diagram of the Matrix Converter is represented in Figure 3.1.

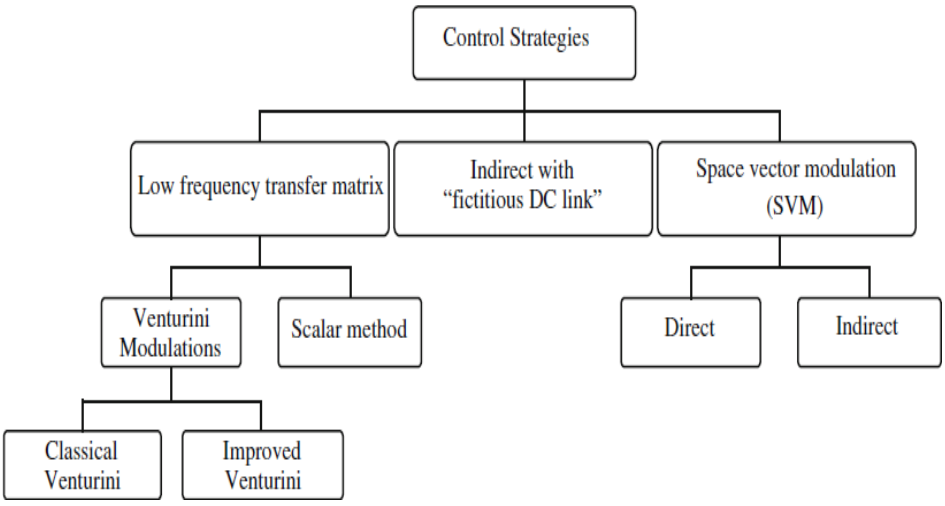

Figure 3.1: Classification of MC Modulation Techniques [26].

3.2 Modulation Techniques

The concept of switching functions [27] is used to derive a mathematical model of the Matrix Converter. Ideal switching is assumed in this analysis. The switching function, S_{Kj}, is defined as the representation of the switch connecting input line *K* to output line *j*.

When the switch is ON, the switching function has a value of 1 and when the switch is OFF, the switching function has a value of 0. The input terminals of the converter are connected to the three-phase input voltages v_a , v_b, and v_c. The three phase desired output voltages v_A, v_B, and v_C of the converter are obtained using Equations 3.1 and 3.2. The same thing for the currents.

$$\begin{bmatrix} v_a(t) \\ v_b(t) \\ v_c(t) \end{bmatrix} = \begin{bmatrix} S_{Aa(t)} & S_{Ba(t)} & S_{Ca(t)} \\ S_{Ab(t)} & S_{Bb(t)} & S_{Cb(t)} \\ S_{Ac(t)} & S_{Bc(t)} & S_{Cc(t)} \end{bmatrix} \begin{bmatrix} v_A(t) \\ v_B(t) \\ v_C(t) \end{bmatrix} \tag{3.1}$$

$$\begin{bmatrix} i_A(t) \\ i_B(t) \\ i_C(t) \end{bmatrix} = \begin{bmatrix} S_{Aa(t)} & S_{Ab(t)} & S_{Ac(t)} \\ S_{Ba(t)} & S_{Bb(t)} & S_{Bc(t)} \\ S_{Ca(t)} & S_{Cb(t)} & S_{Cc(t)} \end{bmatrix} \begin{bmatrix} i_a(t) \\ i_b(t) \\ i_c(t) \end{bmatrix} \tag{3.2}$$

One of the most important rules that Matrix Converters must obey is the one expressed by Equation 3.3.

$$\sum_{k=A,B,C} S_{ka}\ (t) \quad = \sum_{k=A,B,C} S_{kb}\ (t) = \sum_{k=A,B,C} S_{kc}\ (t) = 1 \tag{3.3}$$

A typical switching pattern for Matrix Converter is shown in Figure 3.2. If conventional PWM is employed the switching sequence T_{seq}has a fixed period.

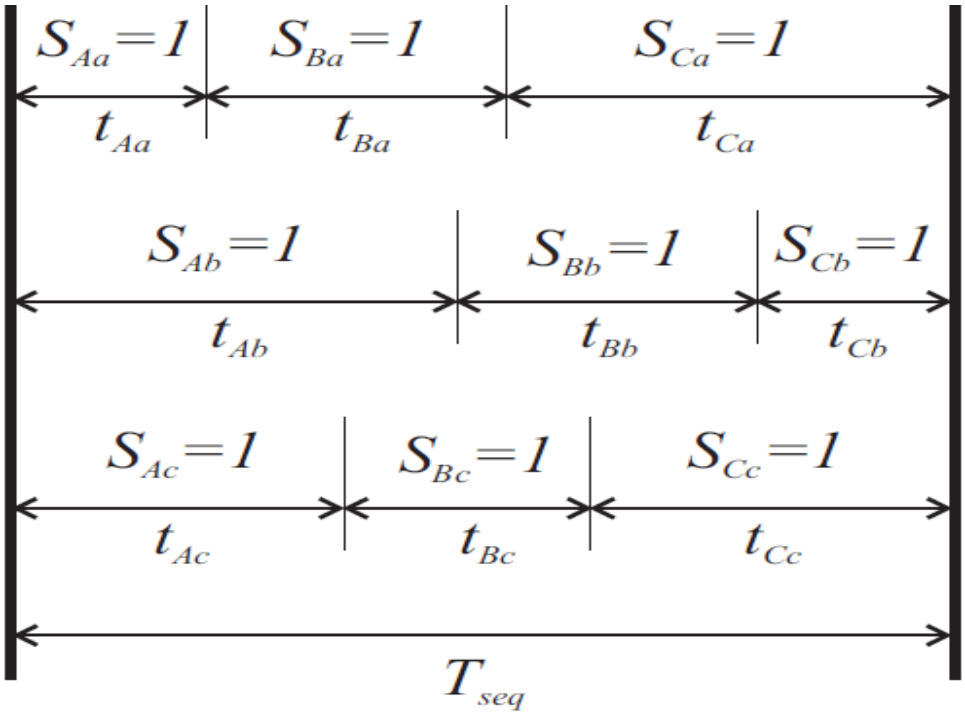

Figure 3.2: General form of Switching Pattern [10].

A modulation duty cycle should be defined for each switch in order to determine the average behavior of the Matrix Converter output voltage waveform. The modulation duty cycle is defined by,

$$m_{Aa}(t) = \frac{t_{Aa}}{T_{seq}} \tag{3.4}$$

Equations 3.5 and 3.6 shows the use of these functions for the three-phase Matrix Converter.

$$\begin{bmatrix} v_a(t) \\ v_b(t) \\ v_c(t) \end{bmatrix} = \begin{bmatrix} m_{Aa(t)} & m_{Ba(t)} & m_{Ca(t)} \\ m_{Ab(t)} & m_{Bb(t)} & m_{Cb(t)} \\ m_{Ac(t)} & m_{Bc(t)} & m_{Cc(t)} \end{bmatrix} \begin{bmatrix} v_A(t) \\ v_B(t) \\ v_C(t) \end{bmatrix} \tag{3.5}$$

$$\begin{bmatrix} i_A(t) \\ i_B(t) \\ i_C(t) \end{bmatrix} = \begin{bmatrix} m_{Aa(t)} & m_{Ab(t)} & m_{Ac(t)} \\ m_{Ba(t)} & m_{Bb(t)} & m_{Bc(t)} \\ m_{Ca(t)} & m_{Cb(t)} & m_{Cc(t)} \end{bmatrix} \begin{bmatrix} i_a(t) \\ i_b(t) \\ i_c(t) \end{bmatrix} \tag{3.6}$$

Voltages v_a, v_b&v_c and currents i_a, i_b&i_c in Equations 3.5 and 3.6 are now values averaged over the sequence time. In Equation 3.7, which is a representation in a more compact notation of Equations 3.5 and 3.6, the matrix *M(t)* is known as the modulation matrix.

$$[v_o(t)] = [M(t)][v_i(t)];\ [i_i(t)] = [M(t)]^T[i_o(t)] \tag{3.7}$$

Using this nomenclature, the constraint equation for Matrix Converters can now be written as,

$$\sum_{k=A,B,C} m_{ka}(t) = \sum_{k=A,B,C} m_{kb}(t) = \sum_{k=A,B,C} m_{kc}(t) = 1 \tag{3.8}$$

3.3 Control Strategies

The modulation problem assumes that a set of sinusoidal output voltages,$v_o(t)$, and input currents, $i_i(t)$;are required. These sets can be represented as,

$$[v_i(t)] = V_{im}\begin{bmatrix}\cos(\omega_i t)\\ \cos\left(\omega_i t + \frac{2\pi}{3}\right)\\ \cos\left(\omega_i t + \frac{4\pi}{3}\right)\end{bmatrix} \tag{3.9}$$

$$[i_o(t)] = I_{om}\begin{bmatrix}\cos(\omega_o t + \phi_o)\\ \cos\left(\omega_i t + \phi_o + \frac{2\pi}{3}\right)\\ \cos\left(\omega_i t + \phi_o + \frac{4\pi}{3}\right)\end{bmatrix} \tag{3.10}$$

The aim is to find a modulation matrix, *M*(*t*), such that Equations 3.9 and 3.10 are satisfied, as well as the constraint Equation 3.8.

$$[v_o(t)] = q\ V_{im}\begin{bmatrix}\cos(\omega_o t)\\ \cos\left(\omega_o t + \frac{2\pi}{3}\right)\\ \cos\left(\omega_o t + \frac{4\pi}{3}\right)\end{bmatrix} \tag{3.11}$$

$$[i_i(t)] = q\frac{\cos\phi_o}{\cos\phi_i} I_{om}\begin{bmatrix}\cos(\omega_i t + \phi_i)\\ \cos\left(\omega_i t + \phi_i + \frac{2\pi}{3}\right)\\ \cos\left(\omega_i t + \phi_i + \frac{4\pi}{3}\right)\end{bmatrix} \tag{3.12}$$

In Equations 3.11 and 3.12 q is the voltage transfer ratio, ω_i and $\omega_o$are the input andoutput frequencies and $\phi_i$and $\phi_o$are the input and output phase displacement angles respectively.

3.3.1 Venturini's Method

The problem was treated by Venturini, who found two solutions [25]. The solutions are expressed in Equations 3.13 and 3.14.

$$[M1(t)] = \frac{1}{3}\begin{bmatrix} 1+2\,\mathrm{qcos}(\omega_m t) & 1+2\,\mathrm{qcos}\left(\omega_m t-\frac{2\pi}{3}\right) & 1+2\,\mathrm{qcos}\left(\omega_m t-\frac{4\pi}{3}\right) \\ 1+2\,\mathrm{qcos}\left(\omega_m t-\frac{4\pi}{3}\right) & 1+2\,\mathrm{qcos}(\omega_m t) & 1+2\,\mathrm{qcos}\left(\omega_m t-\frac{2\pi}{3}\right) \\ 1+2\,\mathrm{qcos}\left(\omega_m t-\frac{2\pi}{3}\right) & 1+2\,\mathrm{qcos}\left(\omega_m t-\frac{4\pi}{3}\right) & 1+2\,\mathrm{qcos}(\omega_m t) \end{bmatrix} \tag{3.13}$$

With $\omega_m = (\omega_o - \omega_i)$

$$[M2(t)] = \frac{1}{3}\begin{bmatrix} 1+2\,\mathrm{qcos}(\omega_m t) & 1+2\,\mathrm{qcos}\left(\omega_m t-\frac{2\pi}{3}\right) & 1+2\,\mathrm{qcos}\left(\omega_m t-\frac{4\pi}{3}\right) \\ 1+2\,\mathrm{qcos}\left(\omega_m t-\frac{2\pi}{3}\right) & 1+2\,\mathrm{qcos}\left(\omega_m t-\frac{4\pi}{3}\right) & 1+2\,\mathrm{qcos}(\omega_m t) \\ 1+2\,\mathrm{qcos}\left(\omega_m t-\frac{4\pi}{3}\right) & 1+2\,\mathrm{qcos}(\omega_m t) & 1+2\,\mathrm{qcos}\left(\omega_m t-\frac{2\pi}{3}\right) \end{bmatrix} \tag{3.14}$$

With $\omega_m = (\omega_o + \omega_i)$

If both solutions are combined, the result provides the means for input displacement factor control.

$$[M(t)] = \alpha_1[M1(t)] + \alpha_2[M2(t)] \tag{3.15}$$

where $\alpha_1 + \alpha_2 = 1$

If $\alpha_1 = \alpha_2$ is used, the modulation functions can be expressed in a compact equation:

$$m_{Aa}(t) = \frac{t_{kj}}{T_{seq}} = \frac{1}{3}\left(1 + \frac{2v_k V_j}{V^2_{im}}\right) \tag{3.16}$$

For $K = A;B;C$ and $j = a;\ b;\ c$

Where V_{im} is the average input voltage.

The modulation algorithm represented by Equation 3.16 is suitable for real time implementation but in practice it is not used due to the 50% voltage transfer ratio limitation.

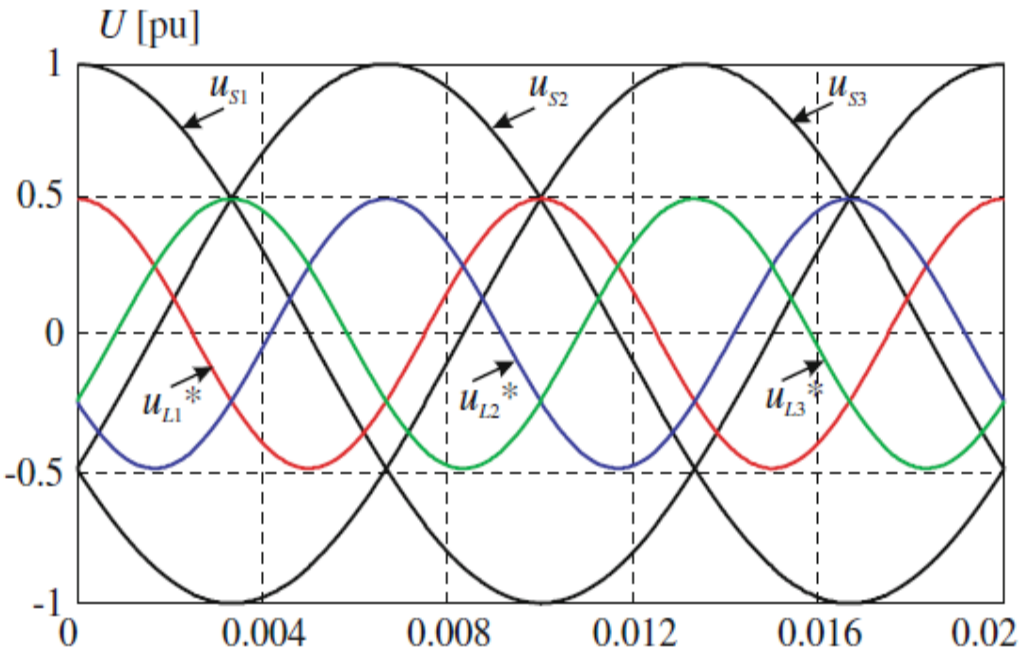

Figure3.3: Maximum Voltage Ratio of 0.5 for Classical Venturini Modulation [26].

3.3.2 Venturini's Optimum Method

The target output voltages in Equation 3.11 are modified in order to include the third harmonics. The maximum theoretical output to input voltage ratio, *q*, can be increased up to 86%, as shown in Equation 3.17.

$$[v_o(t)] = qV_{im}\begin{bmatrix} \cos(\omega_o t) - \frac{1}{6}\cos(3\omega_o t) + \frac{1}{2\sqrt{3}}\cos(3\omega_i t) \\ \cos\left(\omega_o t + \frac{2\pi}{3}\right) - \frac{1}{6}\cos(3\omega_o t) + \frac{1}{2\sqrt{3}}\cos(3\omega_i t) \\ \cos\left(\omega_o t + \frac{4\pi}{3}\right) - \frac{1}{6}\cos(3\omega_o t) + \frac{1}{2\sqrt{3}}\cos(3\omega_i t) \end{bmatrix} \quad (3.17)$$

Note that triple harmonics in the input frequency as well as in the output frequency are added. According to [28], when unity displacement factor is required the Equation 3.16 becomes,

$$m_{kj} = \frac{1}{3}\left[1 + \frac{2v_k V_j}{V^2{}_m} + \frac{4q}{3\sqrt{3}}\sin(\omega_i t + \beta_k)\sin(3\omega_i t)\right] \quad (3.18)$$

β_k= 0,$\frac{2\pi}{3}$, $\frac{4\pi}{3}$ .for K=A,B,C respectively.

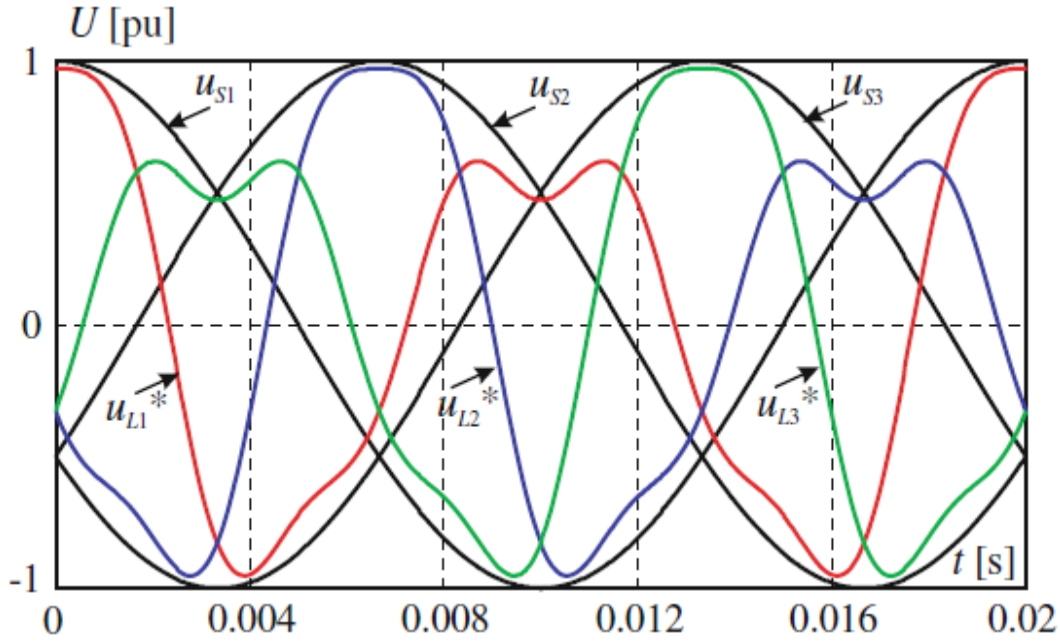

Figure 3.4: Illustrating Maximum Voltage Ratio of 0.866 for Venturini's Improved Modulation for f_L= 100Hz[26].

3.3.3 Scalar Method

In 1987 G. Roy proposed a scalar control algorithm for [24]. The modulation duty cycle for this method is given by

$$m_{kj} = \frac{(v_j - v_M)v_K}{1.5\,V^2_{im}}$$

$$m_{Lj} = \frac{(v_j - v_M)v_L}{1.5\,V^2_{im}} \tag{3.19}$$

$$m_{Mj} = 1 - (m_{kj} + m_{Lj})$$

For $j = a; b; c$ respectively

The subscript M is assigned to the input voltage which has a different polarity to the other two inputs and the subscript L is assigned to the smallest of the other two input voltage magnitudes. The third input voltage is assigned subscript K. As in the previous method, the common-mode addition is used in order to modify the target output voltages, v_j . This modification (by adding the third harmonics) is employed to achieve 86% voltage ratio capability. the modulation duty cycles for the scalar method can be represented by Equation 3.20.

$$m_{kj} = \frac{t_{kj}}{T_{seq}} = \frac{1}{3}\left[1 + \frac{2v_k V_j}{V^2_{im}} + \frac{2}{3}\sin(\omega_i t + \beta_k)\sin(3\omega_i t)\right] \tag{3.20}$$

For K=A, B, C and j= a,b,c

βk = 0,$\frac{2\pi}{3}$, $\frac{4\pi}{3}$ .for K=A,B,C respectively.

Equations 3.18 and 3.20 are equal when the output voltage is maximum (q =0.866) The only difference between the methods is that the right most term is used in conjunction with q in the Venturini method and is fixed at its maximum value in the scalar method. The effect on output voltage is negligible except at low switching frequencies, where the Venturini method is superior.

3.3.4 Space Vector Modulation (SVM) Method

The SVM is a control technique that has been widely used in adjustable speed drives. Generally, in conventional DC-link VSI, the SVM technique is used to provide the reference output voltage vectorV_{ref} . This vector is obtainedby basic voltage vectors generated by the different inverter configurations [29].

3.3.4.1 Clarke Transformation

The Clarke transformation transforms a three-phase system into a two-phase orthogonal system.

$$\begin{bmatrix} x_\alpha \\ x_\beta \\ x_0 \end{bmatrix} = \frac{2}{3}\begin{bmatrix} 1 & \frac{1}{2} & -\frac{1}{2} \\ 0 & \sqrt{3} & -\sqrt{3} \\ 1 & 1 & 1 \end{bmatrix}\begin{bmatrix} x_a \\ x_b \\ x_c \end{bmatrix} \tag{3.21}$$

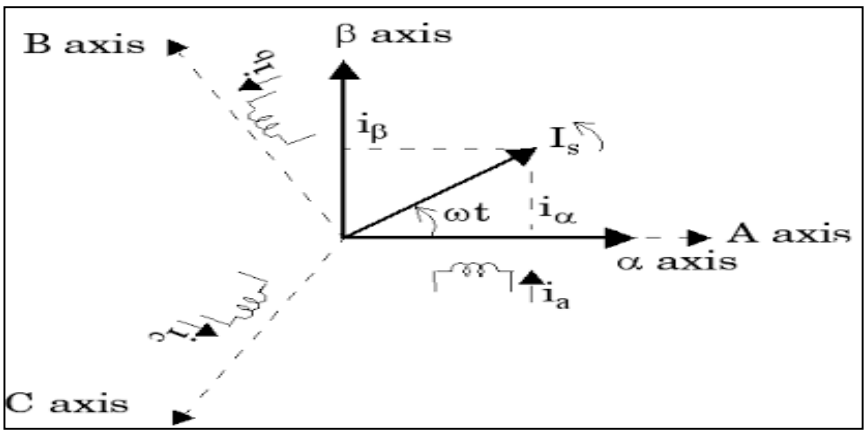

Figure 3.5: Perform Transformation from Three Phase to αβ0 [32].

With $x_\alpha$and $x_\beta$in an orthogonal reference frame and$x_0$the homopolar componentof the system.

3.3.4.2 Modulation Technique Based on the Relative Input Voltages and SVM

The rectifier stage and inverter stage modulation strategy proposed in [30] are presented in this section. A combined modulation strategy will be presented at the end of the section.

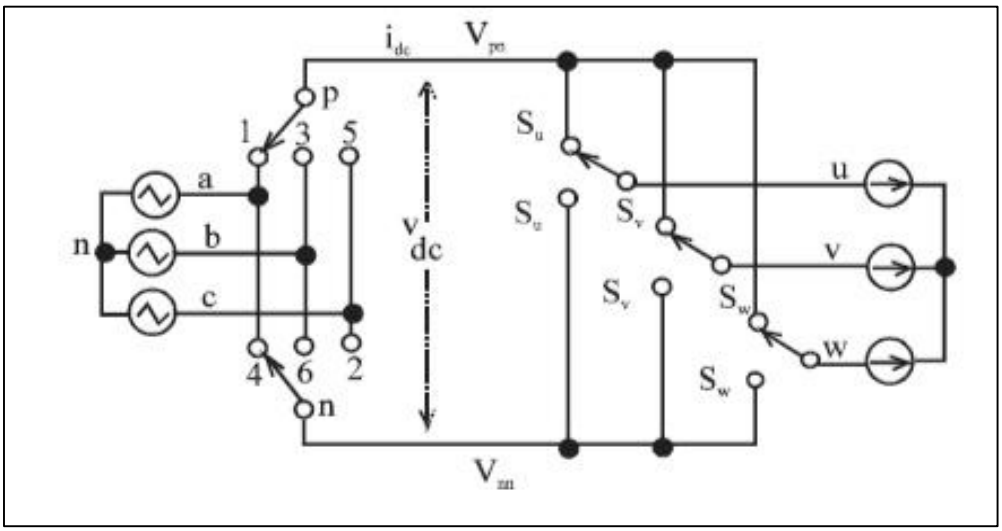

Figure 3.6: Three-Phase AC -AC Indirect Matrix Converter [32].

Consider the indirect matrix converter topology of Figure 3-6. The input terminals of the converter are connected to the three-phase input voltages V_a , V_b, and V_c. The three phase desired output voltages V_A, V_B, and V_C of the converter are obtained using Equation 3-22.

$$\begin{bmatrix} v_a(t) \\ v_b(t) \\ v_c(t) \end{bmatrix} = \begin{bmatrix} S_{Aa(t)} & S_{Ba(t)} & S_{Ca(t)} \\ S_{Ab(t)} & S_{Bb(t)} & S_{Cb(t)} \\ S_{Ac(t)} & S_{Bc(t)} & S_{Cc(t)} \end{bmatrix} \begin{bmatrix} v_A(t) \\ v_B(t) \\ v_C(t) \end{bmatrix} \tag{3.22}$$

Restraining to the condition that says that one and only one switch in each output phase must be conducting, we will obtain twenty seven possible switching combinations [31], those combinations are tabulated below:

Group I: 6 combinations in which each output phase is connected to a different input phase. Both magnitude and phase of the resultant vectors are variable in these cases.

Table 3-1: Six Switching Combinations of the Switches for Three-Phase AC-AC IMC [32].

	Phase connect ion			output line Voltage			Input Phase Current		
I	a	b	c	V_{ab}	V_{ba}	V_{ca}	I_a	I_b	I_c
	a	c	b	$-V_{ca}$	$-V_{bc}$	$-V_{ab}$	I_a	I_c	I_b
	b	a	c	$-V_{ab}$	$-V_{ca}$	$-V_{bc}$	I_b	I_a	I_c
	b	c	a	V_{bc}	V_{ca}	V_{ab}	I_c	I_a	I_b
	c	a	b	V_{ca}	V_{ab}	V_{bc}	I_b	I_c	I_a
	c	b	a	$-V_{bc}$	$-V_{ab}$	$-V_{ca}$	I_c	I_b	I_a

Group II: 18 combinations where the output voltage and the input current vectors have fixed directions with magnitudes that vary with the input voltage phase angle and the output current phase angle respectively. These combinations result when any two output phases are connected to the same input phase.

Table 3-2: 18 Switching Combinations of the Switches for Three-Phase AC-AC SMC [32].

II	A	a	c	c	$-V_{ca}$	0	V_{ca}	I_a	0	$-I_a$
		b	c	c	V_{bc}	0	$-V_{bc}$	0	I_a	$-I_a$
		b	a	a	$-V_{ab}$	0	V_{ab}	$-I_a$	I_a	0
		c	a	a	V_{ca}	0	$-V_{ca}$	$-I_a$	0	I_a
		c	b	b	$-V_{bc}$	0	$-V_{ca}$	0	$-I_a$	I_a
		a	b	b	V_{ab}	0	$-V_{ab}$	I_a	$-I_a$	0
		c	a	c	V_{ca}	$-V_{ca}$	0	I_b	0	$-I_b$
		c	b	c	$-V_{bc}$	V_{bc}	0	0	I_b	$-I_b$
		a	b	a	V_{ab}	$-V_{ab}$	0	$-I_b$	I_b	0
	B	a	c	a	$-V_{ca}$	V_{ca}	0	$-I_b$	0	I_b
		b	c	b	V_{bc}	$-V_{bc}$	0	0	$-I_b$	I_b
		b	a	b	$-V_{ab}$	V_{ab}	0	I_b	$-I_b$	0
	C	c	c	a	0	V_{ca}	$-V_{ca}$	I_c	0	$-I_c$
		c	c	b	0	$-V_{bc}$	V_{bc}	0	I_c	$-I_c$
		a	a	b	0	V_{ab}	$-V_{ab}$	$-I_c$	I_c	0
		a	a	c	0	$-V_{ca}$	V_{ca}	$-I_c$	0	I_c
		b	b	c	0	V_{bc}	$-V_{bc}$	0	$-I_c$	I_c
		b	b	a	0	$-V_{ab}$	V_{ab}	I_c	$-I_c$	0

Group II: 3 combinations giving null output voltage and input current vectors. All three output phases are connected to the same input phase in these combinations.

Table 3-3: 3 Switching Combinations of the Switches for Three-Phase AC-AC IMC [32].

III	a	a	a	0	0	0	0	0	0
	b	b	b	0	0	0	0	0	0
	c	c	c	0	0	0	0	0	0

Equation 3-22 can be reduced into a two-stage converter as given by Equation 3-23 and 3-24.

$$\begin{bmatrix} V_p \\ V_n \end{bmatrix} = \begin{bmatrix} S_{ap} & S_{bp} & S_{cp} \\ S_{an} & S_{bn} & S_{cn} \end{bmatrix} * \begin{bmatrix} V_a \\ V_b \\ V_c \end{bmatrix} \tag{3.23}$$

$$\begin{bmatrix} V_A \\ V_B \\ V_C \end{bmatrix} = \begin{bmatrix} S_{ap} & S_{An} \\ S_{Bp} & S_{Bn} \\ S_{Cp} & S_{Cn} \end{bmatrix} * \begin{bmatrix} V_p \\ V_n \end{bmatrix} \tag{3.24}$$

The given input source voltages and the assumed output currents are:

$$\begin{bmatrix} V_a \\ V_b \\ V_c \end{bmatrix} = V_{im} \begin{bmatrix} \cos(\omega_i t) \\ \cos\left(\omega_i t + \frac{2\pi}{3}\right) \\ \cos\left(\omega_i t + \frac{4\pi}{3}\right) \end{bmatrix} = V_{im} \begin{bmatrix} \cos(\theta_a) \\ \cos(\theta_b) \\ \cos(\theta_c) \end{bmatrix} \tag{3.25}$$

$$\begin{bmatrix} i_A \\ i_B \\ i_C \end{bmatrix} = I_{om} \begin{bmatrix} \cos(\omega_o t + \phi_o) \\ \cos\left(\omega_i t + \phi_o + \frac{2\pi}{3}\right) \\ \cos\left(\omega_i t + \phi_o + \frac{4\pi}{3}\right) \end{bmatrix} \tag{3.26}$$

A. Modulation Technique of the Rectifier Stage

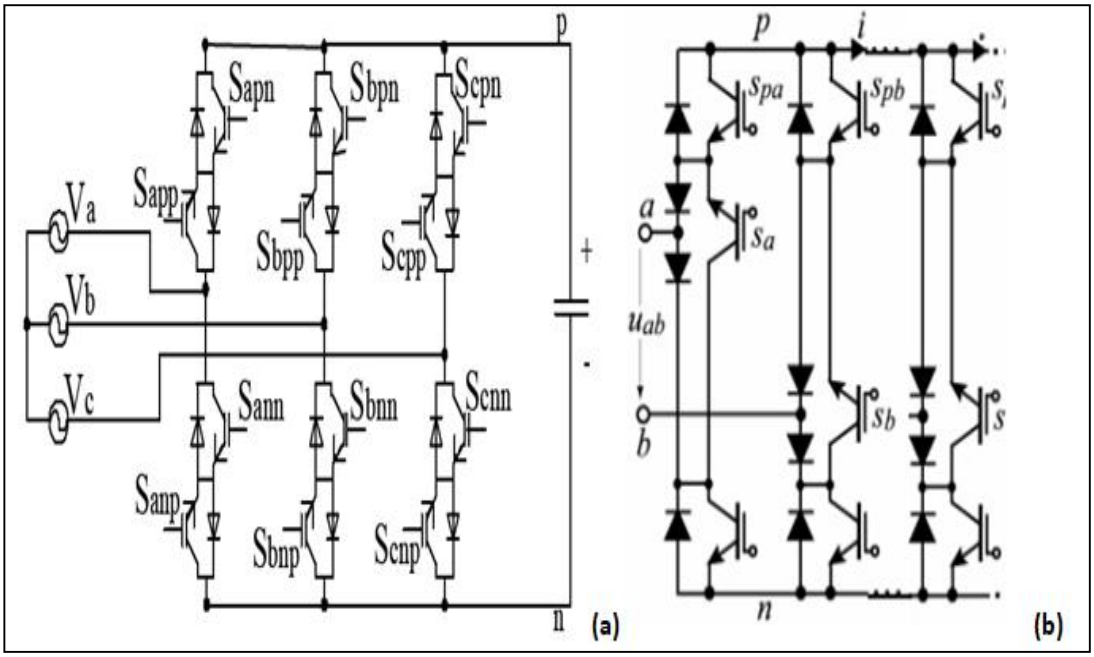

Figure 3.7: A Standalone Rectifier Converter (a) IMC; (b) SMC [32].

The modulation strategy applied to control the rectifier switches ensures a constant DC voltage is provided to the inverter side of the converter. This strategy is presented as follows:

Six switching intervals based on the line side voltage

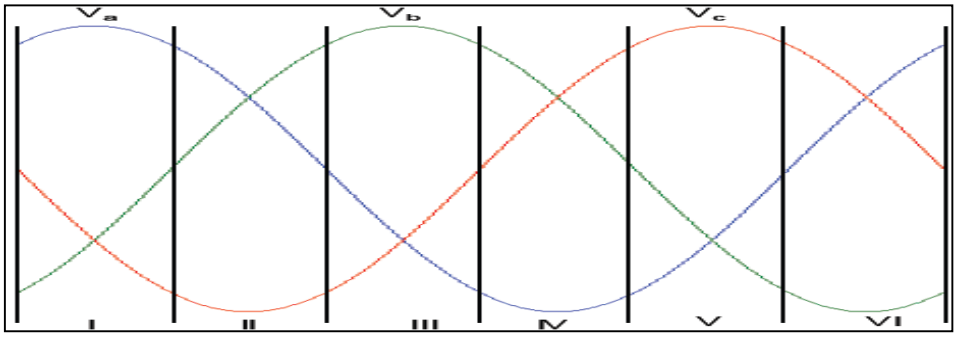

Figure 3.8: Six Intervals Based on the Input Synchronization Angle [32].

Two portions in each switching cycle

Portion I: Switches S_{ap} , S_a ,S_{bn} , and S_b are turned on, and the rest of the line side switches are turned off. The DC voltage $V_{pn}$is then equal to the line voltage V_{ab} , and the DC current i_{pn} of the rectifier is equal to i_a and $-i_b$. Thecurrent $i_c$equals zero, since the switches are turned off. The duty cycle of this portion is defined as:

$$d_{ba} = \frac{-V_b}{V_a} = \frac{-\cos(\theta_b)}{\cos(\theta_a)} \quad (3.27)$$

The constant DC voltage V_{pn}during this first portion is given as[32]:

$$V_{pn}=d_{ba}*V_{ab}= d_{ba}*(V_a-V_b) \quad (3.28)$$

Portion II: The switches S_{ap}, S_a ,S_{cn} , and $S_c$are turned on and the rest of theline side switches are turned off. The DC voltage $V_{pn}$is then equal to the line voltage V_{ac} , and the DC current $i_{pn}$of the rectifier is equal to $i_a$and–i_c . Thecurrenti$_b$ equals zero, since the switches are turned off. The duty cycle of this portion is defined as:

$$d_{ca} = \frac{-V_c}{V_a} = \frac{-\cos(\theta_c)}{\cos(\theta_a)} \quad (3.29)$$

The constant DC voltage V_{pn}during this second portion is given as:

$$V_{pn}=d_{ca}*V_{ac}= d_{ca}*(V_a-V_c) \quad (3.30)$$

The constant DC voltage V_{pn} provided by the rectifier converter stage for a given switching period T_s is:

$$V_{pn}=d_{ba}*V_{ab}+ d_{ca}*V_{ac} \quad (3.31)$$

Where: $d_{ba}+ d_{ca}= 1$

Substituting Equation 3-24, 3-25, and 3-30 in 3-31 will result in Equation 3-32:

$$V_{pn} = \frac{3}{2\left|\cos\theta a\right|} V_{im} \quad (3.32)$$

The figure 3.9 shows a phase input is clamped to positive or negative DC link bus in $\frac{\pi}{3}$ wide intervals when the corresponding phase voltage does show the highest absolute value.

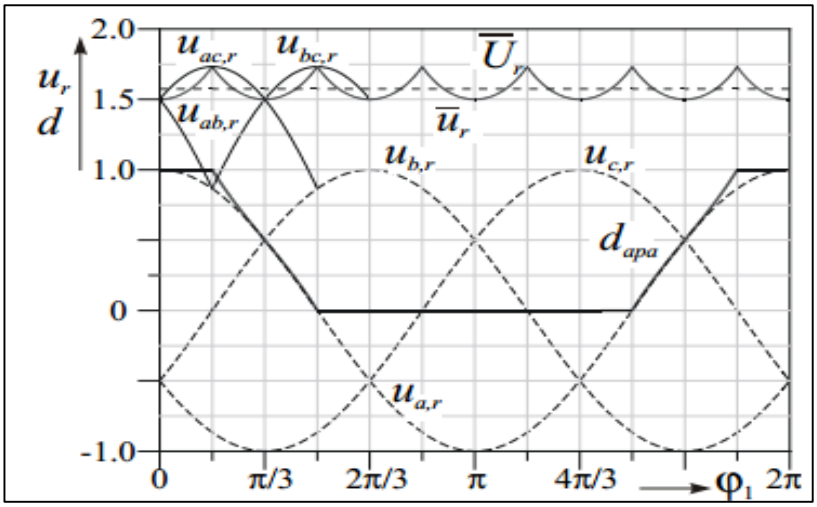

Figure 3.9: Time Behavior of the Input Phase Voltages and the Local Averaged DC Link[33].

The table below shows the switching state of the rectifier converter switches and the DC-link voltageV_{pn} provided for the given one cycle of the input synchronization angle.

Table 3-4: The duty cycle, switching state and DC-link voltage determined of the rectifier circuit [32].

Intervals	I		II		III		IV		V		VI	
Input angle θ_a	-π/6 ~ π/6		π/6 ~ π/2		π/2 ~ 5π/6		5π/6~ 7π/6		7π/6~3π/2		11π/2~ -π/6	
Duty cycle	d_{ba}	d_{ca}	d_{ac}	d_{bc}	d_{cb}	d_{ab}	d_{ba}	d_{ca}	d_{ac}	d_{bc}	d_{cb}	d_{ab}
Conducting switches	S_{ap}		S_{cn}		S_{bp}		S_{an}		S_{cp}		S_{bn}	
	S_{bn}	S_{cn}	S_{ap}	S_{bp}	S_{cn}	S_{an}	S_{bp}	S_{cp}	S_{bn}	S_{an}	S_{ap}	S_{cp}
DC voltage	V_{ab}	V_{ab}	V_{ab}	V_{ab}	V_{ab}	V_{ab}	V_{ab}	V_{ab}	V_{ab}	V_{ab}	V_{ab}	V_{ab}

B. Modulation Technique of the Inverter Stage

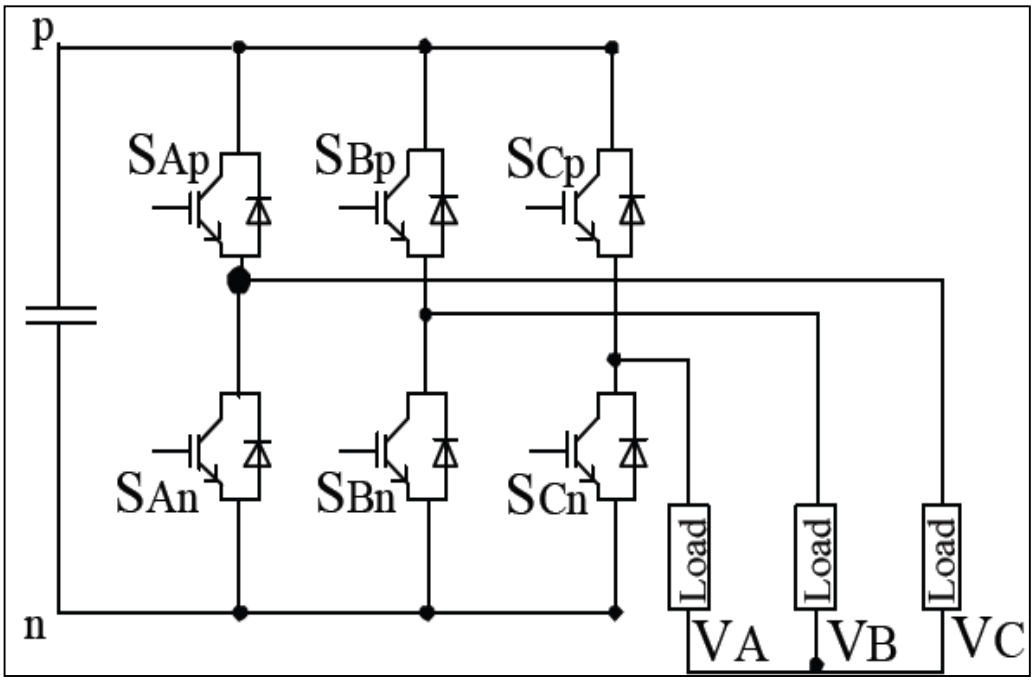

Figure 3.10: An Inverter Stage Circuit [32].

The first six combinations produce non-zero output voltages and are known as the non-zero switching states. Whereas the remaining two combinations are zero output voltages, and are known as the zero switching states.

The resulting space vector of the desired output line voltages is given by Equation 3-33.

$$V_{\text{ref}}=V_{AB}+V_{BC}\,e^{j2\pi/3}+V_{CA}\,e^{j-2\pi/3} \tag{3.33}$$

Voltage vectors V_1 – V_6 are of the same magnitude displaced by 60° as shown in Figure 3-11. The remaining vectors, V_0 and V_7, are zero magnitude voltage vectors placed at the origin of the $\alpha - \beta$ plane.

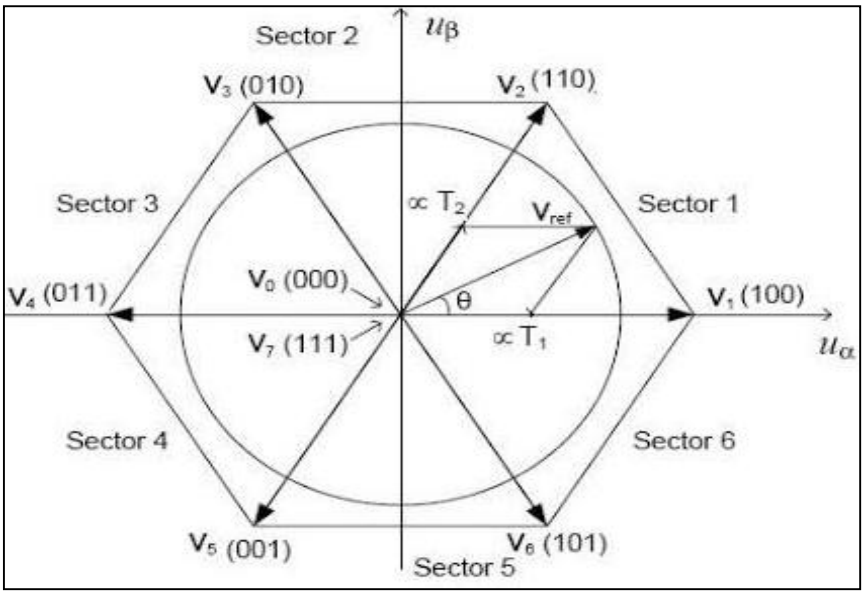

Figure 3.11: The Active Switching State Vectors and the Six Sectors of SVM [32].

Suppose the angle θ_0 is in the sector I, the vector reference V_{ref}can be approximatedby two adjacent non-zero switching state vector voltages V_1 and V_2. A zero switching state vector voltage V_0 or $V_7$is also added to improve the magnitude of the voltage vector.

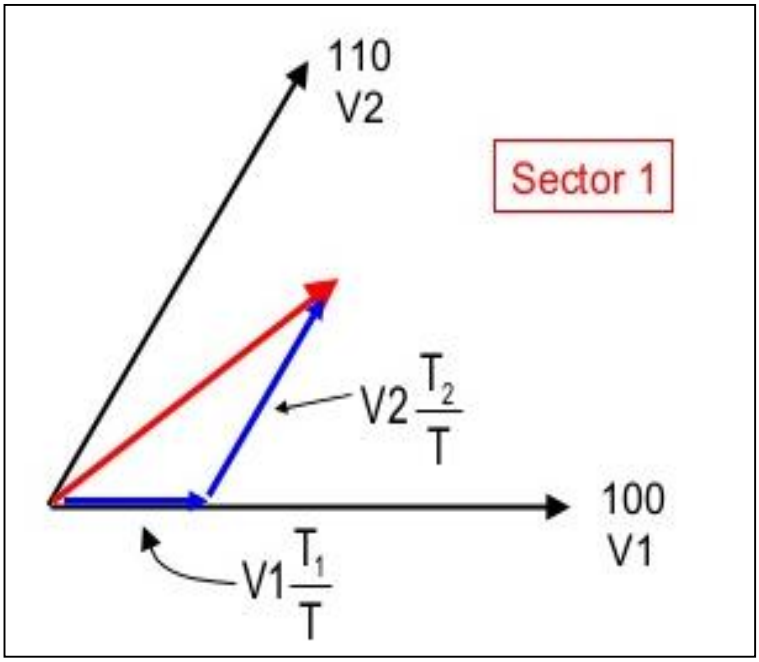

Figure 3.12: Duty Cycle and Adjacent Vector Voltage [32].

The calculation of the dwell time:

$$V_{ref}*T_S = T_1*V_1 + T_2*V_2 + T_0*V_0$$

$$T_S = T_1 + T_2 + T_0$$

$$T_1 = \frac{V_{ref}\sin(60-\alpha)}{V_{DC}\sin(60)}T_S \quad (3.34)$$

$$T_2 = \frac{V_{ref}\sin(\alpha)}{V_{DC}\sin(60)}T_S$$

$$T_0 = T_s - T_1 - T_2$$

The duty cycles d_α,d_β are :

$$d_\alpha = \frac{T_1}{T_{seq}} \; ; \qquad d_\beta = \frac{T_2}{T_{seq}}$$

$$V_{ref} = d_\alpha*V_1 + d_\beta*V_2 \quad (3.35)$$

The corresponding duty cycles of the non-zero active state voltages and the zero state voltages are:

$$d_\alpha = \frac{2}{\sqrt{3}}k\sin(\frac{\pi}{3}-\theta)$$

$$d_\beta = k\sin(\theta) \quad (3.36)$$

$$d_0 = 1 - d_\alpha - d_\beta$$

If the desired output space vector voltage is in sector I and the synchronization input phase angle is in interval I, the duty cycles are calculated as:

During the first portion,

$$d_1 = d_\alpha*\mathrm{d_{ba}}$$

$$d_2 = d_\beta*\mathrm{d_{ca}} \quad (3.37)$$

$$d_0 = 1 - d_1 - d_2$$

The switching time corresponding to the calculated duty cycle is given as the product of the duty cycle and the switching period T_s.

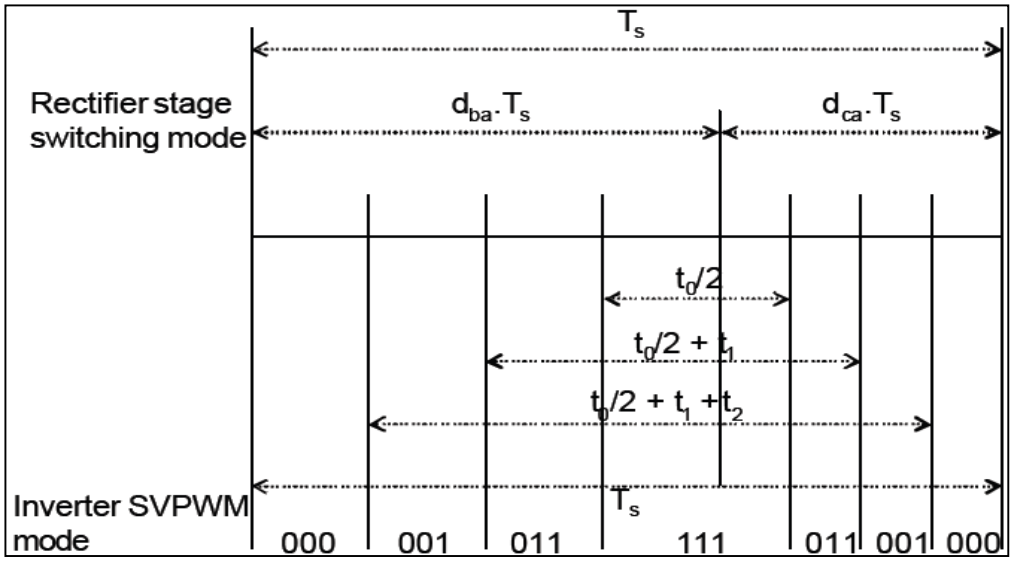

Figure 3.13: PWM Sequence of the Indirect Matrix Converter [32].

The line side switches commutate at both the beginning and end of each portion. If a zero vector is selected for the inverter on the load side at this time, then the line side switches can commutate at zero current [30]. Figure 3-13 shows the PWM sequence of the converter.

It can be found that the load side VSI utilizes the zero vector, while the line switches are commutating. Hence, at this time instant, all currents on the rectifier side are zero so that zero current commutation can be guaranteed for the line side switches.

3.4 Conclusion

This chapter gave the background of the various different modulation control strategies It has been showed that the output-input transfer ratio can be improved by adding the third harmonic components of the input and desired output voltages to the components of the desired output voltage from 50% to 86.6%.the scalar method and the SVM modulation technique for both rectifier and inverter sides. The proposed commutation strategy based on zero current commutation was presented.

4 Simulation And Results

4.1 Introduction

In this chapter, the simulation of the Sparse Matrix Converter is discussed. In the first part, how to build the simulation model of the Sparse Matrix Converter is built in MATLAB / Simulink is introduced. The simulation model mainly consists of the power circuit and the control circuit. In the second part, the simulation results of the Sparse Matrix Converter are shown and analyzed.

4.2 Design parameters

The parameters of components in the power circuit simulation are specified in Table 4.1

Table 4.1: The Parameters of the Simulation.

Phase_Phase rms voltage	**380 V**
Emmulated DC voltage	V_{DC} **=600V**
Resistive load	R_L **= 100Ω**
inductive load	L**=0.1H**
AC mains frequency	F_N **=50 Hz**
Switching frequency	F_S **=10kHz**
Simulation type	**Discrete**
Sample time	10^{-5} **s**

4.3 Simulation model

The simulation model of the Sparse Matrix Converter can be divided into two main parts, the power circuit, and the control circuit subsystem.

4 Simulation And Results

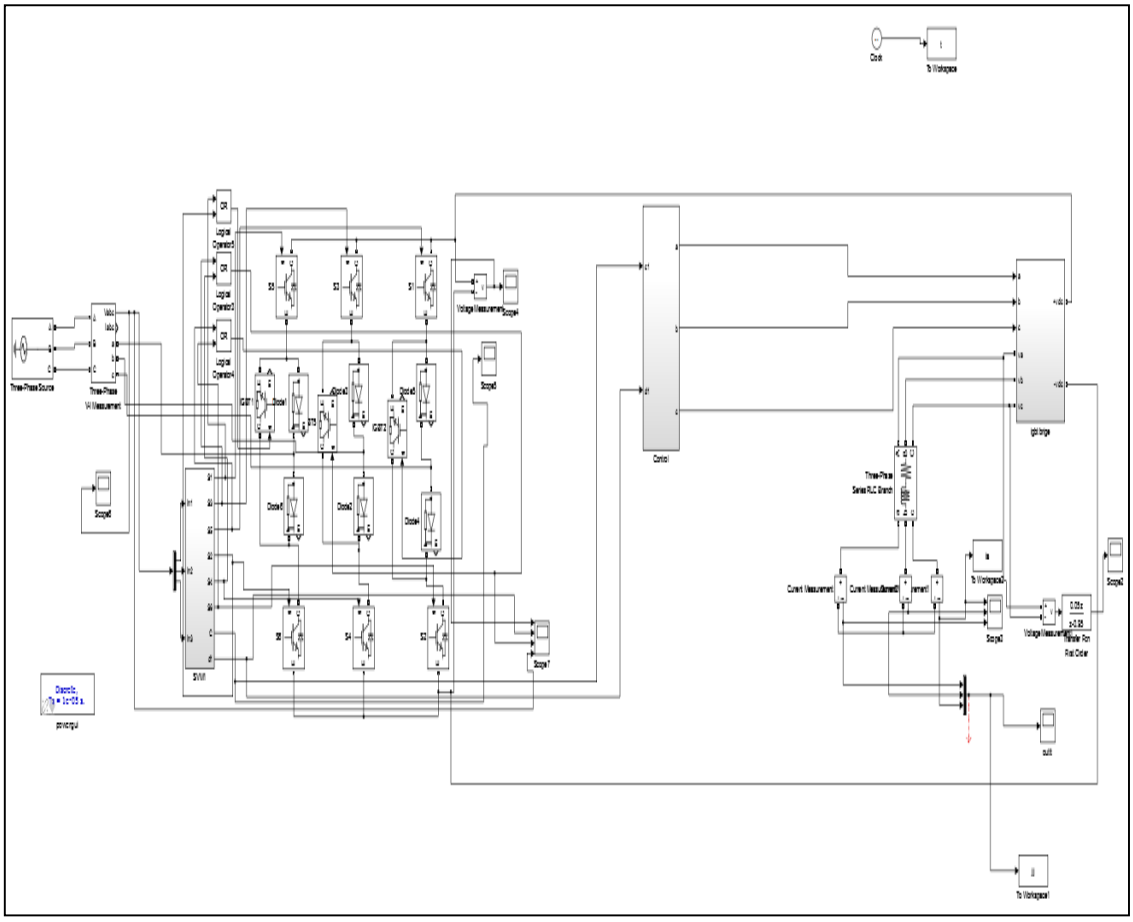

Figure 4.1: Simulink Model of the Matrix Converter.

The general block diagram of the simulation model of the Sparse Matrix Converter is shown in the following block diagram.

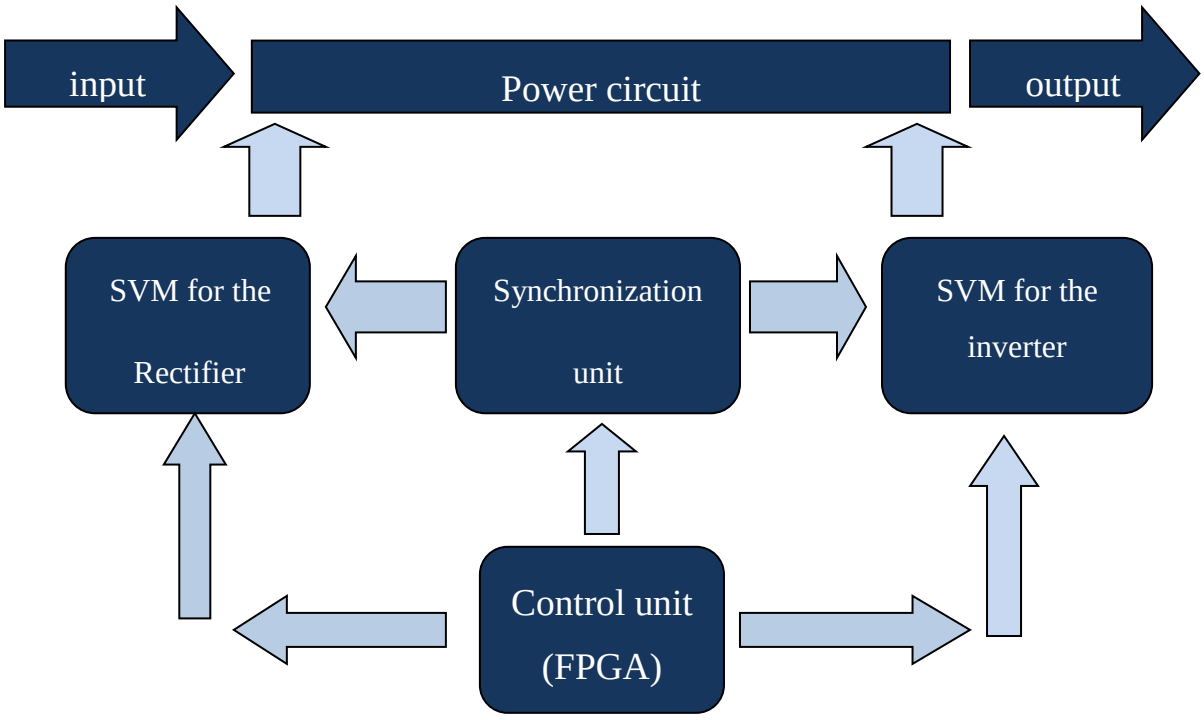

Figure 4.2: General diagram of the System.

4.4 Power circuit simulation model

The power circuit consists of six bi-directional switches in the rectification stage constructed using nine IGBTs and three diodes connected in an antiparallel common emitter configuration, and six unidirectional switches in the inversion stage. Figure 4.3 and 4.4 show the power circuits of the rectification and inversion stages respectively.

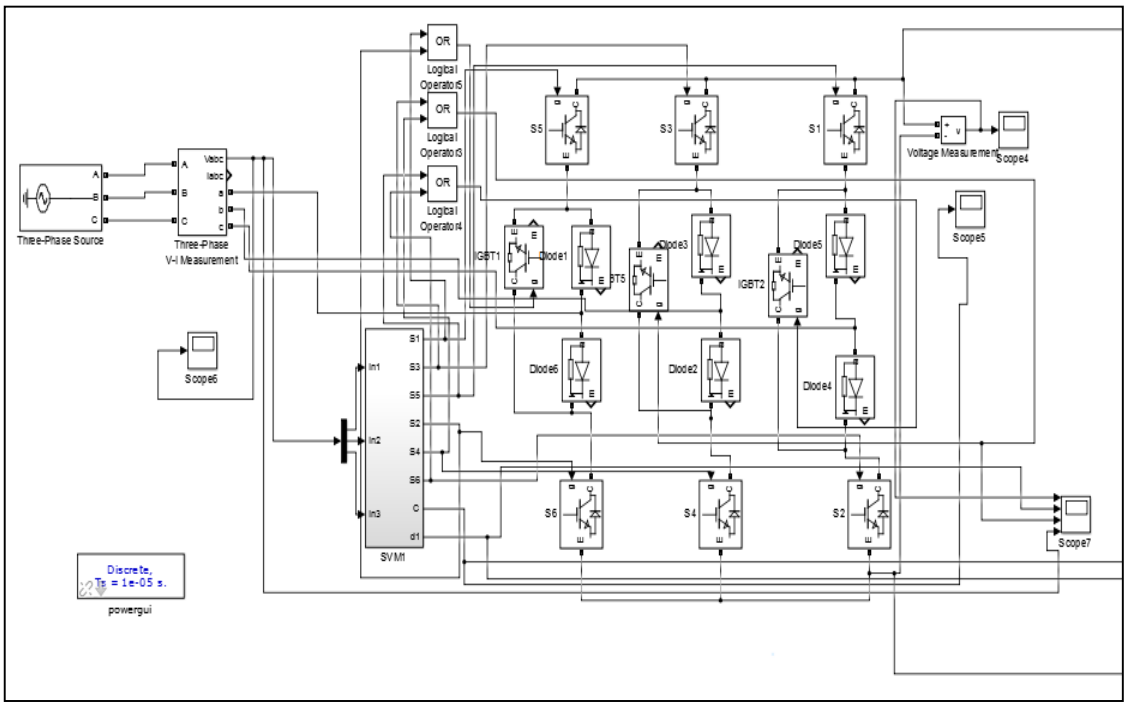

Figure 4.3: Power Circuit for Rectification Stage.

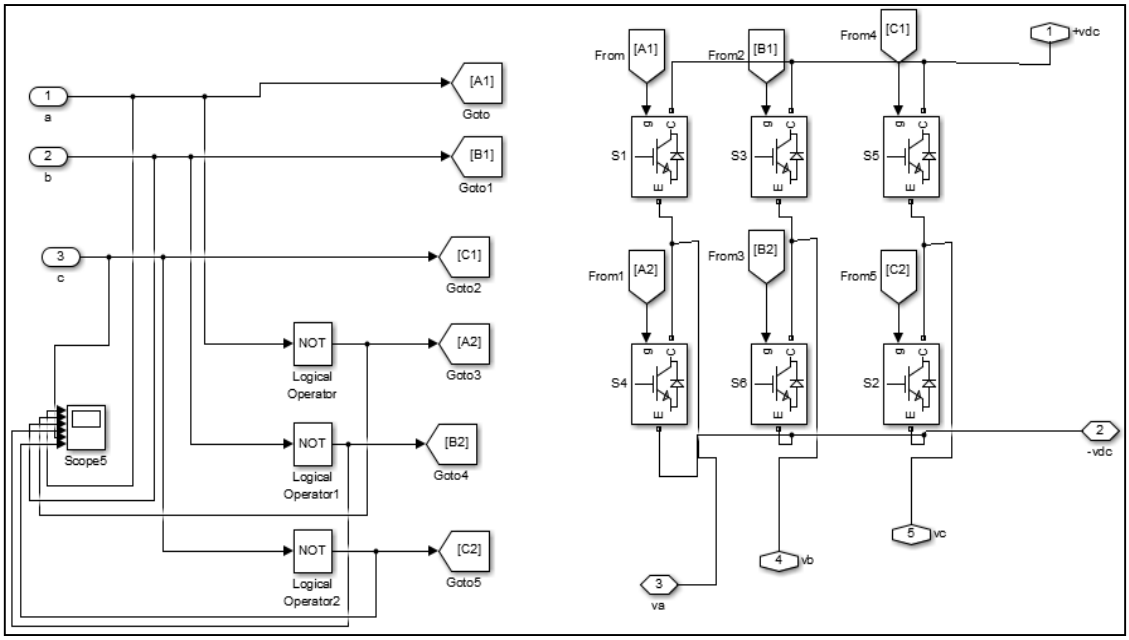

Figure 4.4: Power Circuit for Inversion Stage.

4.5 Control Circuit Simulation Model

In the control part, space vector modulation and zero current commutation technique were used. The control circuit mainly includes two parts; it was constructed using a chain of blocks, each of which performs a specific task in the modulation process, namely the alpha beta transformation, sector identification, switching times calculation and PWM signal generations. Figure 4.5 and 4.6 show the overall control diagrams for both rectification and inversion stages respectively.

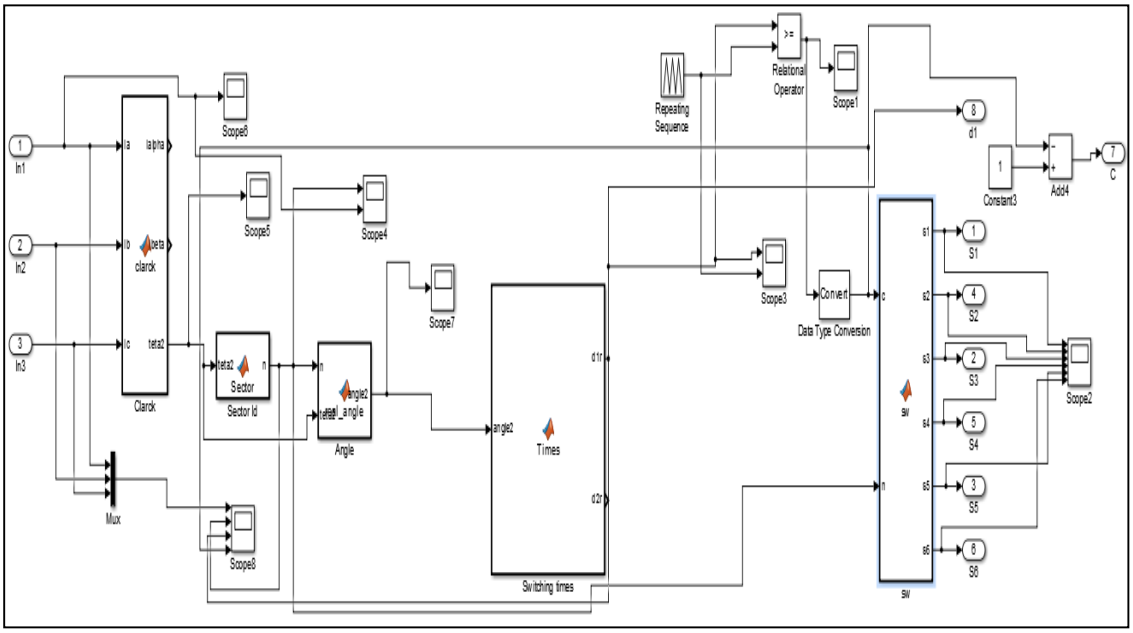

Figure 4.5: Control Diagram for Rectification Stage.

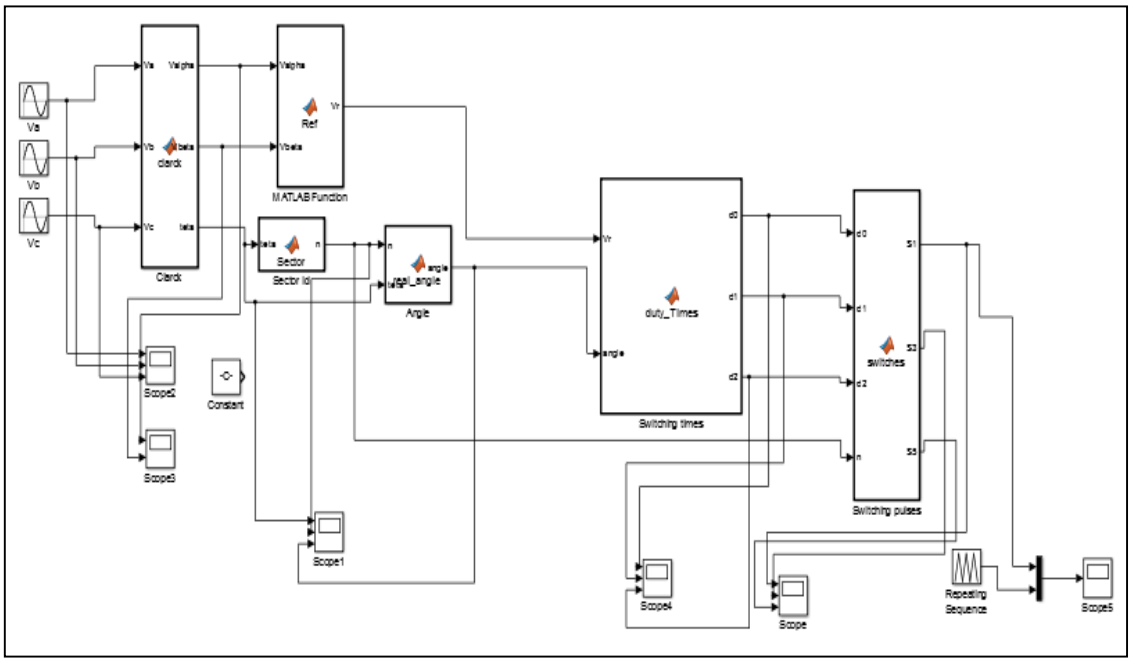

Figure 4.6: Control Diagram for Inversion Stage.

4.6 Simulation Results and Discussion

Figure 4.7 shows the results of the Clarck transformation, we can see the generation of the two voltages shifted by 90deg, namely Vα and Vß, and the angle separating them, those quantities are used to calculate the duty cycles.

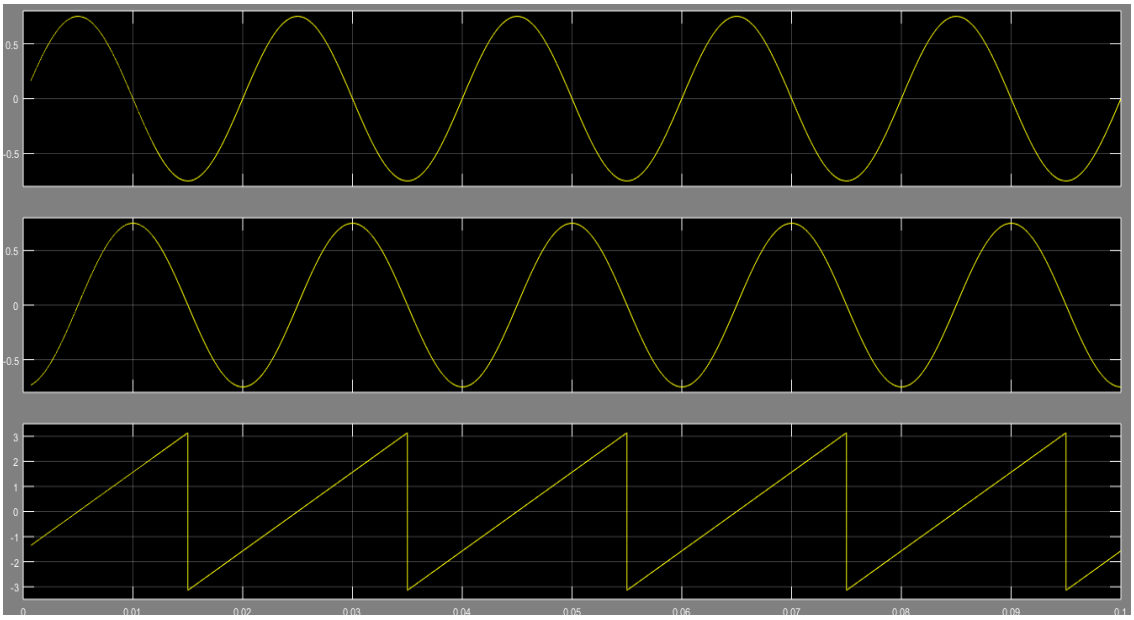

Figure 4.7: Vα, Vß and the angle between Vα and Vß.

Figure 4.8 shows the six sectors of SVM, each sector representing a region of 60°.

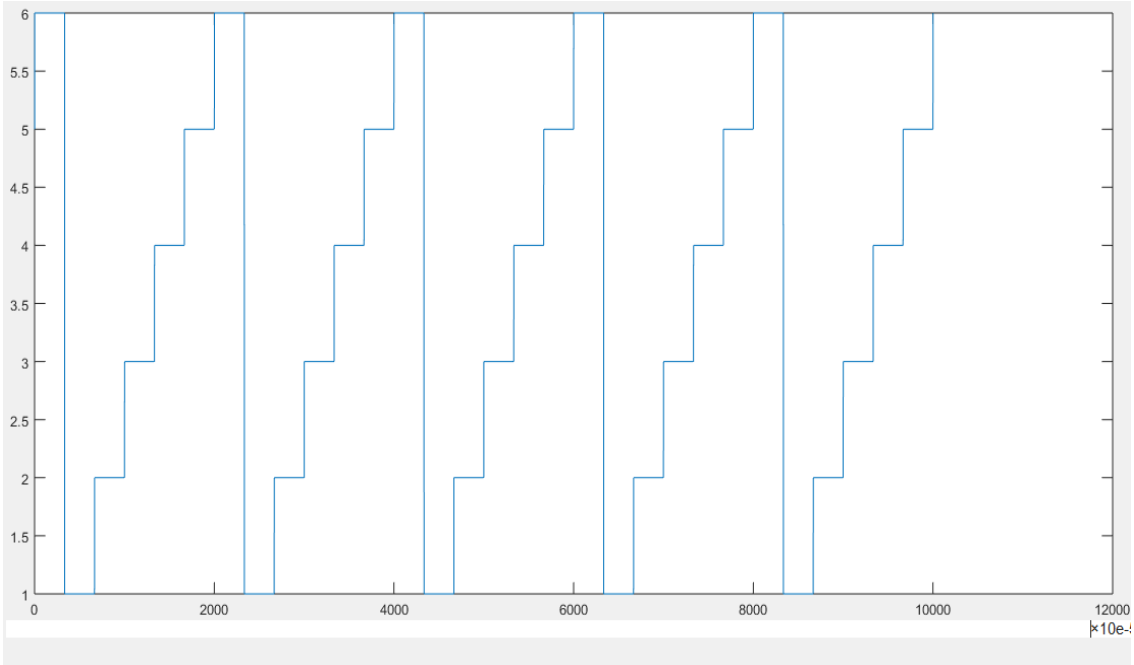

Figure 4.8: The Six Different Sectors of the Space Vector Modulation.

Figure 4.9 shows the zero vector and the generated duty cycles for the two active vectors, used to calculate the switching times.

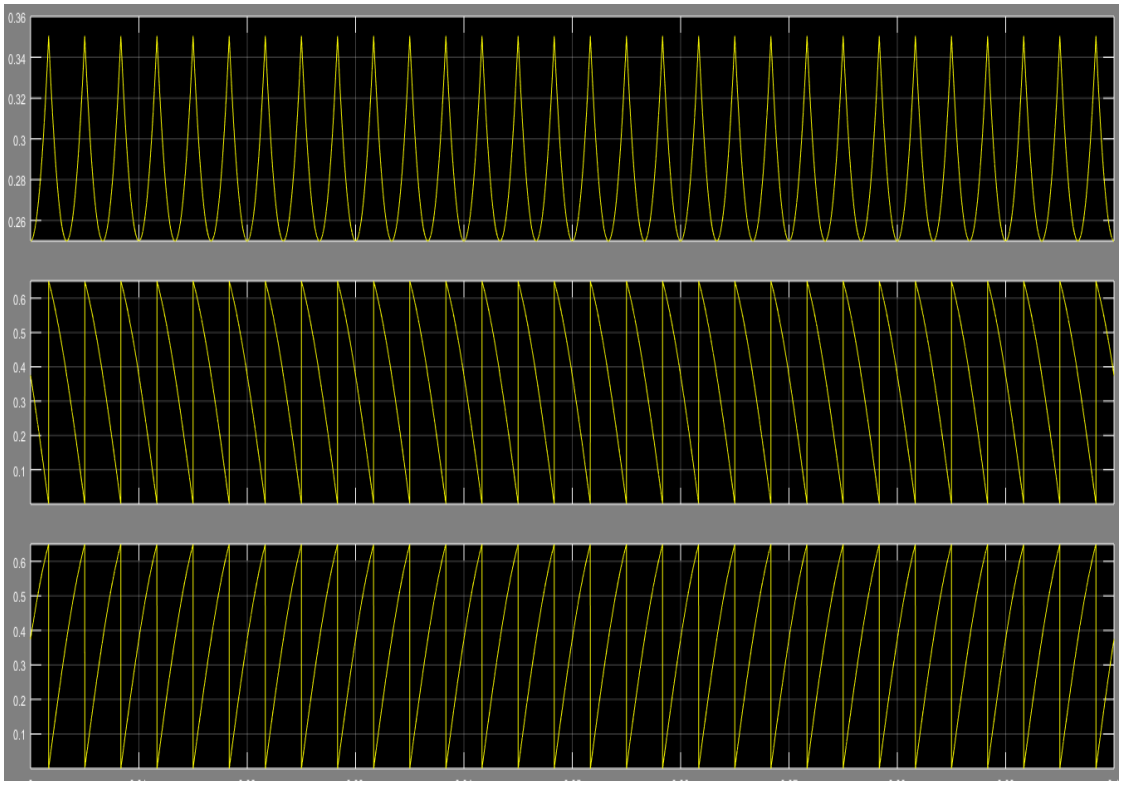

Figure 4.9: The Generated Duty Cycle.

The fundamental components of the switching signals of the SVM obtained using the calculated duty cycles are shown in Figure 4.10. The 120 shift between the three waves can be noticed.

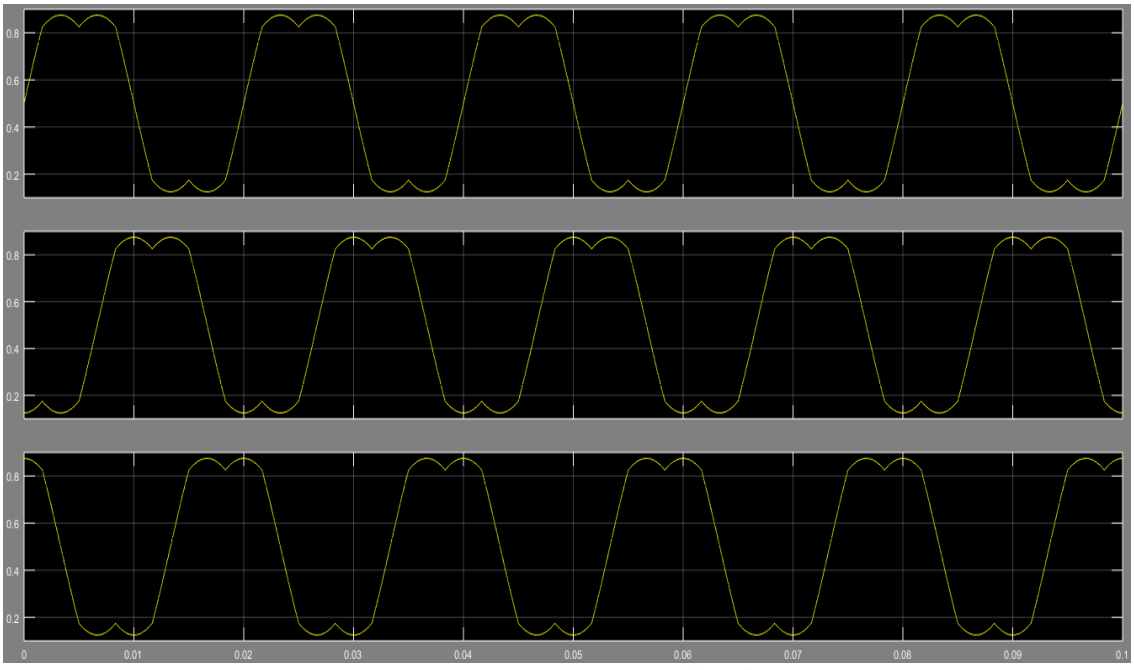

Figure 4.10: SVM Generated Pulses.

4 Simulation And Results

The modulating signals in the rectifier side as mentioned in previous chapters are asymmetric ramp signals, it's a mixture of two antiparallel signals rising and falling inversely proportional, the reason is that the rectifier acts like a "slave" for the inverter side, for that, the modulating signals in the rectifier side must fit the zero vector in the inverter side.

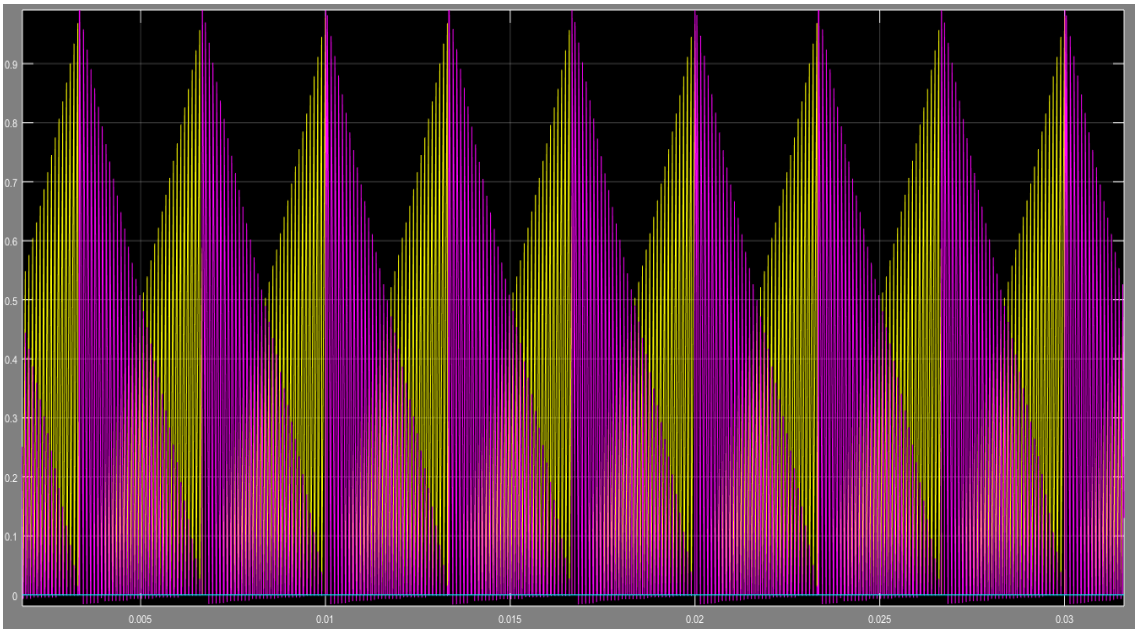

Figure 4.11: Rectifier Side Modulating Signal.

In Figure 4.12 the synchronization between the rectifier stage and the inverter stage is shown, the commutation in the rectifier side occurs when the zero vectors at the inverter side is applied.

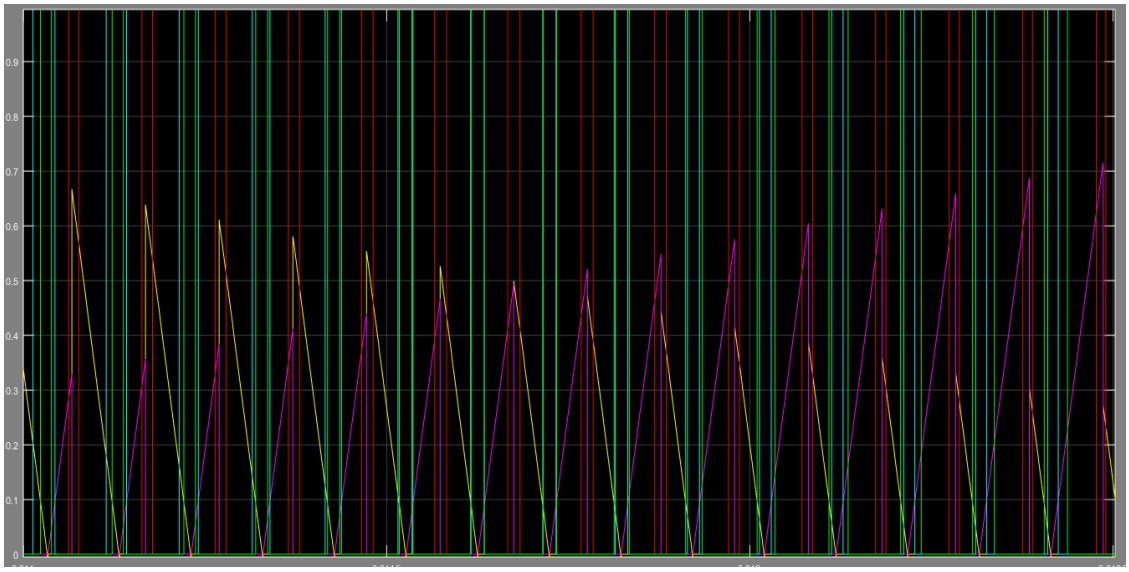

Figure 4.12: Synchronisation Between the Recifier Stage and the Inverter Stage.

Figure 4.13 shows the PWM signals for the six bidirectional switches of the rectifier side

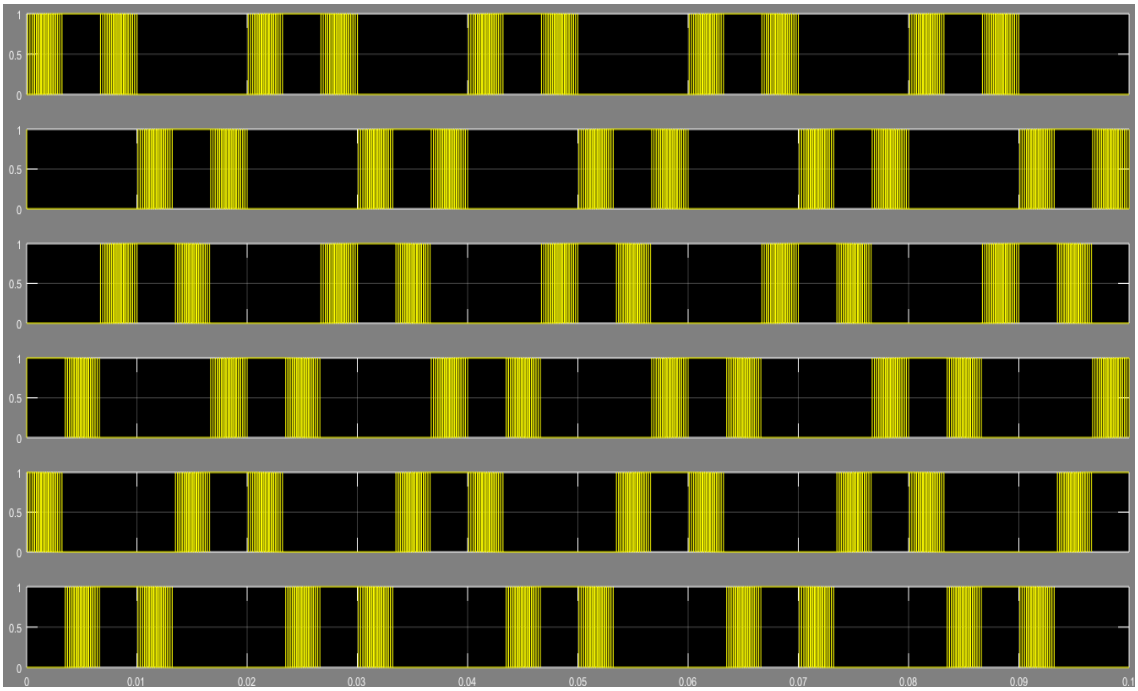

Figure 4.13: the PWM Signals for Six Bidirectional Switches of the Rectifier Side.

In figure 4.14 the DC voltage obtained from the rectifier side is shown, we can see that its value is 3/2 of the input voltage as proposed in the literature.

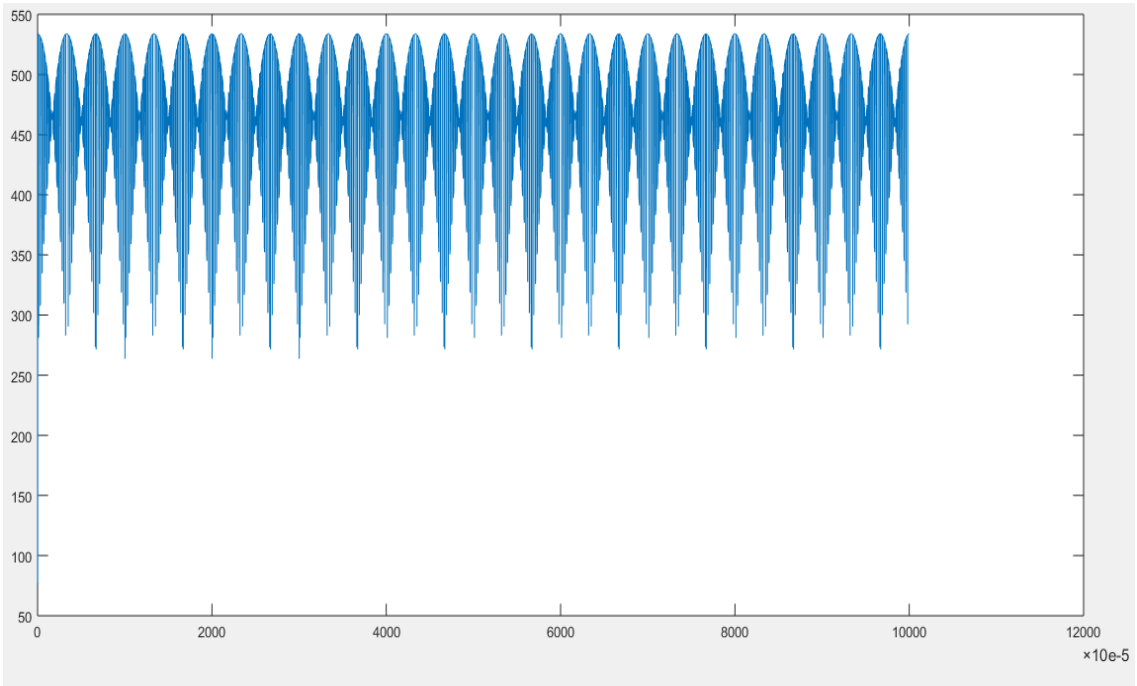

Figure 4.14: DC Voltage from the Rectifier Side.

Figure 4.15 shows the obtained three phase voltages from a 600 V emulated DC bus with modulation index m=0.5. The figure 4.15 verifies the SVM technique.

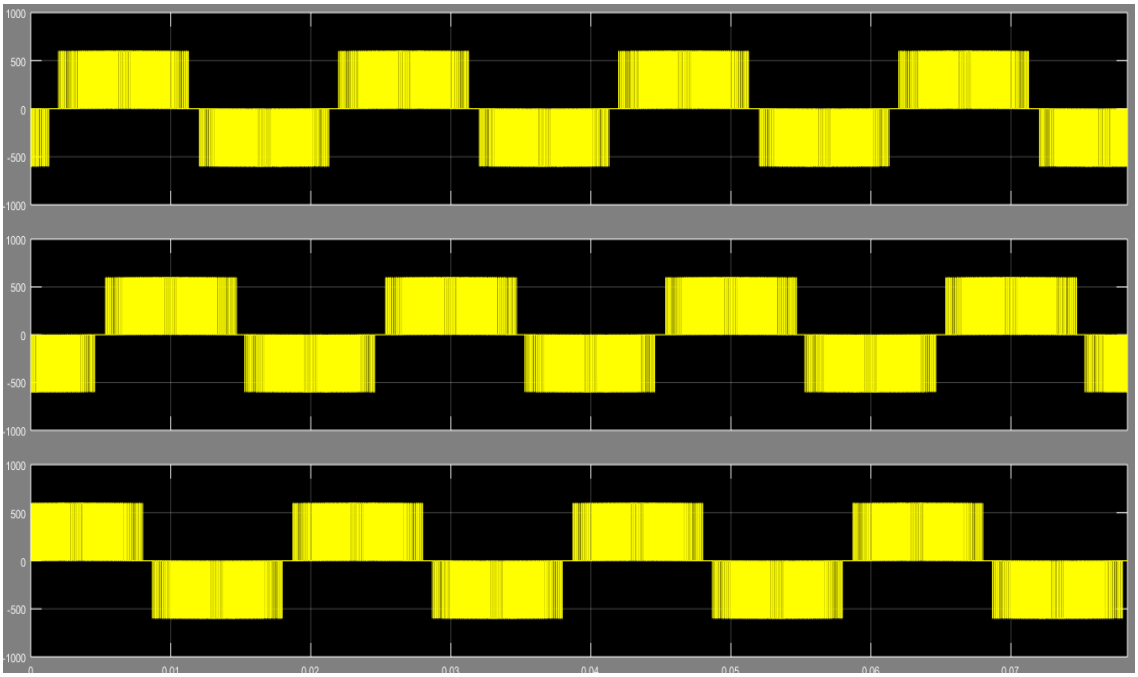

Figure 4.15: Obtained Three Phase Voltages From a Fixed DC Source.

The DC voltage obtained from the rectification will be inverted. Figure 4.16 shows the output current generated using the SVM technique, the three phase currents are shifted by 120 deg.

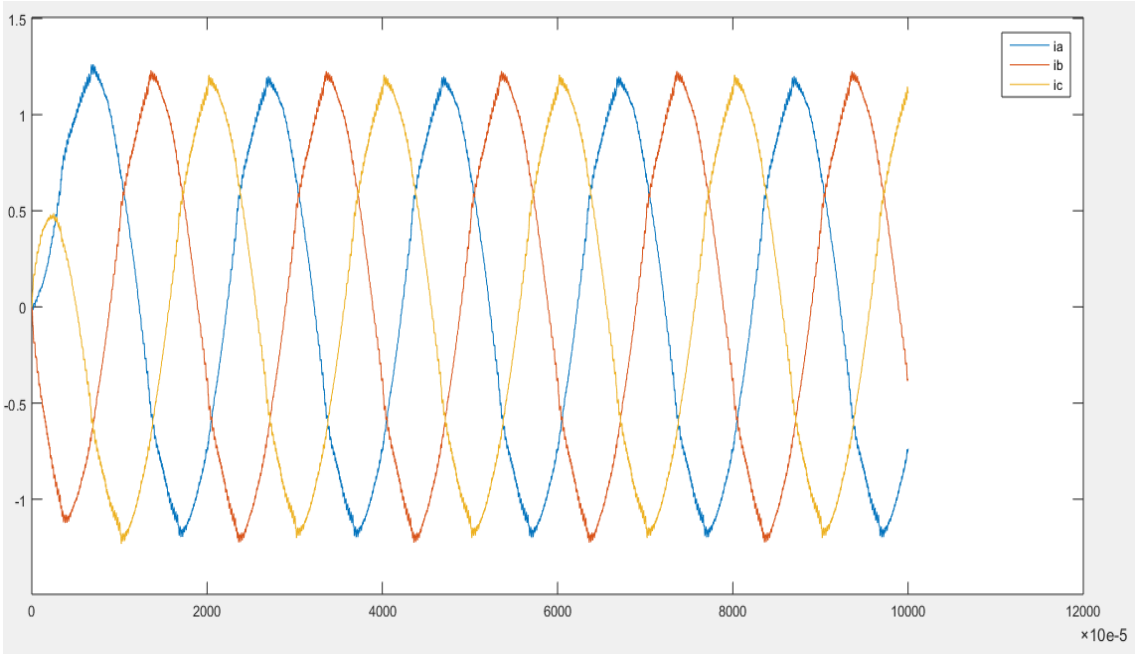

Figure 4.16: The Three Phase Output Currents.

Using the FFT analyzer, we analyzed the total harmonic distortion (THD) of the generated signal. Figure 4.17 shows a low total harmonic distortion (THD) of 6.10 %.

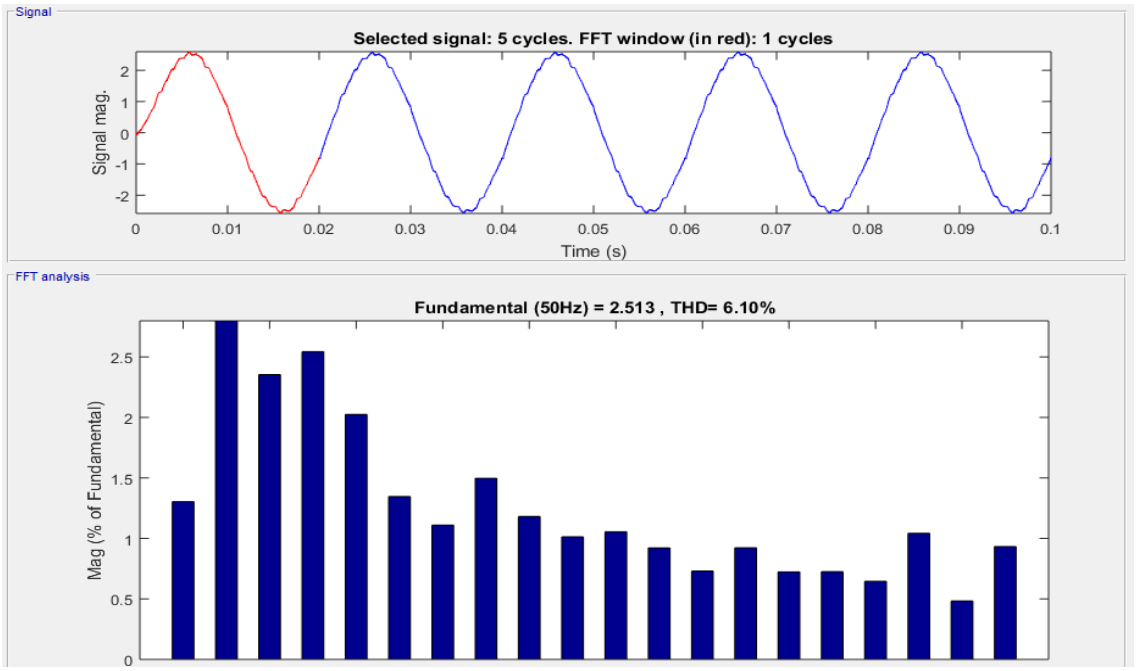

Figure 4.17: FFT Analysis of the Current Waveform.

4.7 Conclusion

In this chapter, simulation of the Sparse Matrix Converter was conducted, Power and Control circuits of both rectification and inversion stages where presented, the use of the SVM technique for the PWM signals generation was shown. Also, various signals representing different quantities where shown, namely the clarck transformation equivalent sinusoidal waves, duty cycles, arrangement of the sectors, and switching pulses and output current and voltage emulated from the rectified DC signal to verify the space vector modulation technique.

Finally, a total harmonic distortion study was performed to show the low THD contained in the current signal; indeed, this particularity is one of the advantages of SVM technique.

5 Implementation And Results

5.1 Introduction

Practical experiments are always essential to prove the theoretical analysis results and simulation results of a power electronics system. In this chapter, the experiments are carried out on realization of the Sparse Matrix Converter, the hardware design and software design of SMC is demonstrated. Experiment results are shown and analyzed as well.

5.2 General Procedure of the Implementation

Generally, the implementation of the circuit is gone through in three main stages where the first is building the power circuitry that will be responsible for generating the power signals, then designing and implementing the gate driving circuitry along with the power supplies, which represent the electronic part of the whole circuit along with the FPGA ,then ending up by programming the FPGA kit by writing the VHDL code that will be able to generate the desired pulses to control the commutations in both rectifier and inverter sides.

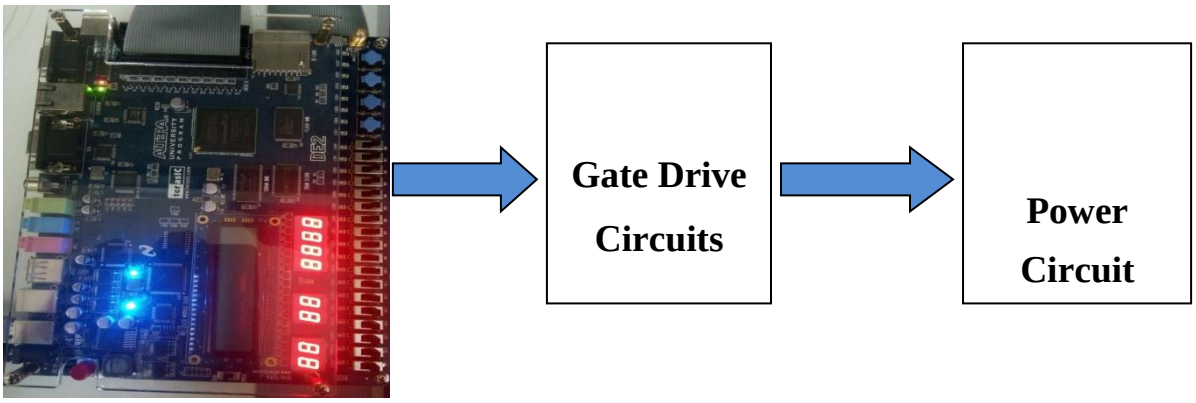

Figure 5.1: General Procedure Followed to Implement the SMC.

5.3 Software part

Commutation system must be controlled. Using Quartus, a VHDL code is written to control each leg for both rectifier and inverter sides. A block is generated from this VHDL code compiled and uploaded into the FPGA DE2 board. The signal is injected into the circuit; from the GPIO pins to the power circuit passing by the gate drives.

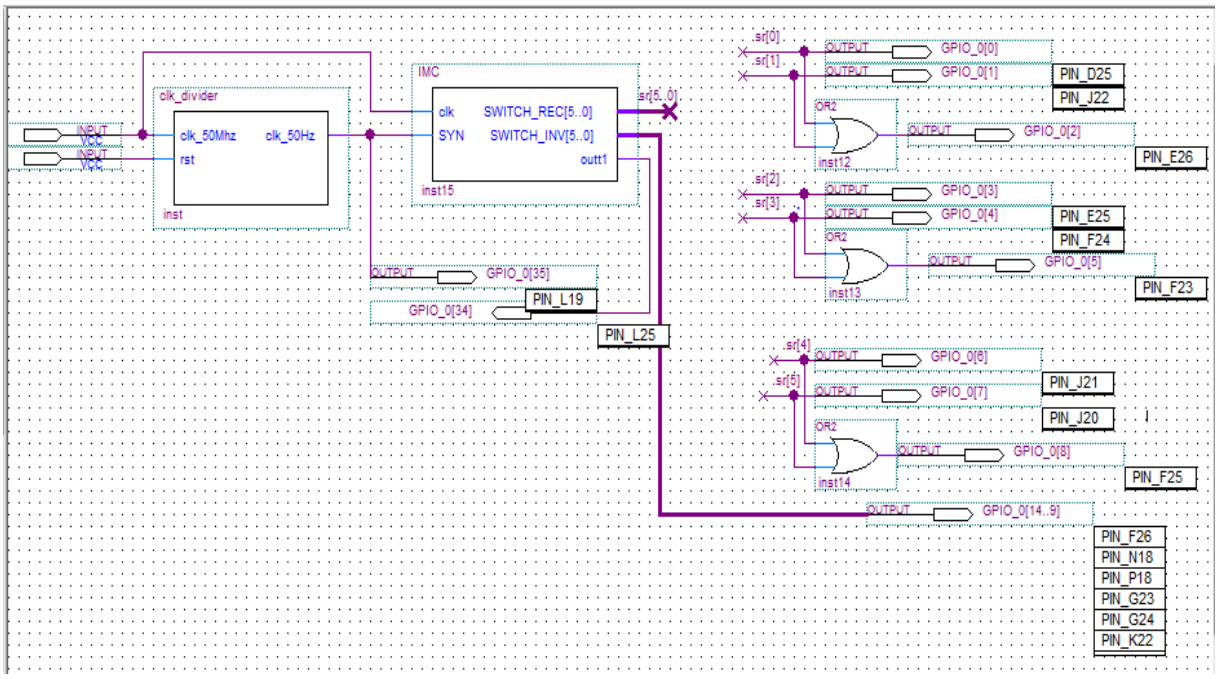

Figure 5.2: The Block Generated from the VHDL Code.

In order to visualize the signals generated from the FPGA, the VHDL code is compiled in Modelsim. Figures 5.3, 5.4 shows the sectors, angles and switches of the rectifier and inverter respectively.

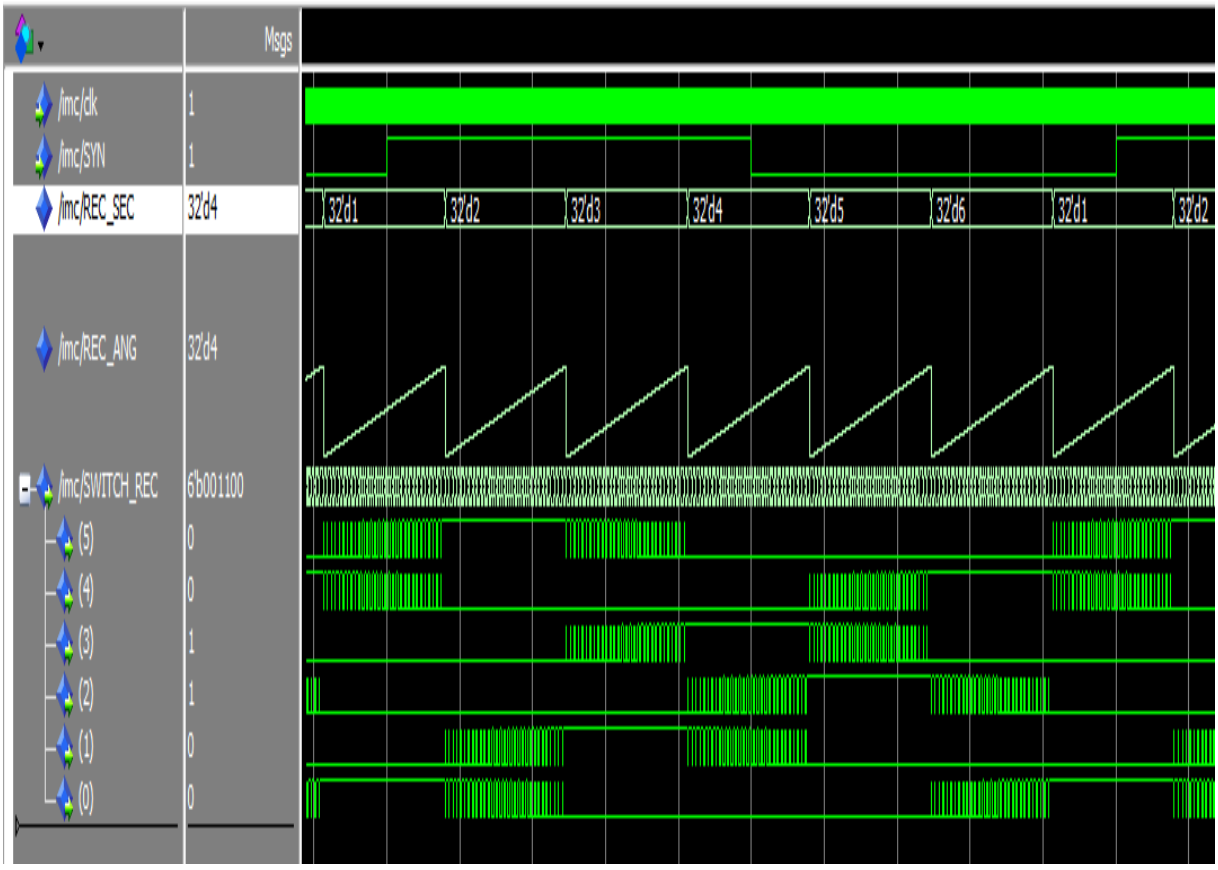

Figure 5.3: Angles, Sectors and Switches of the Rectifier.

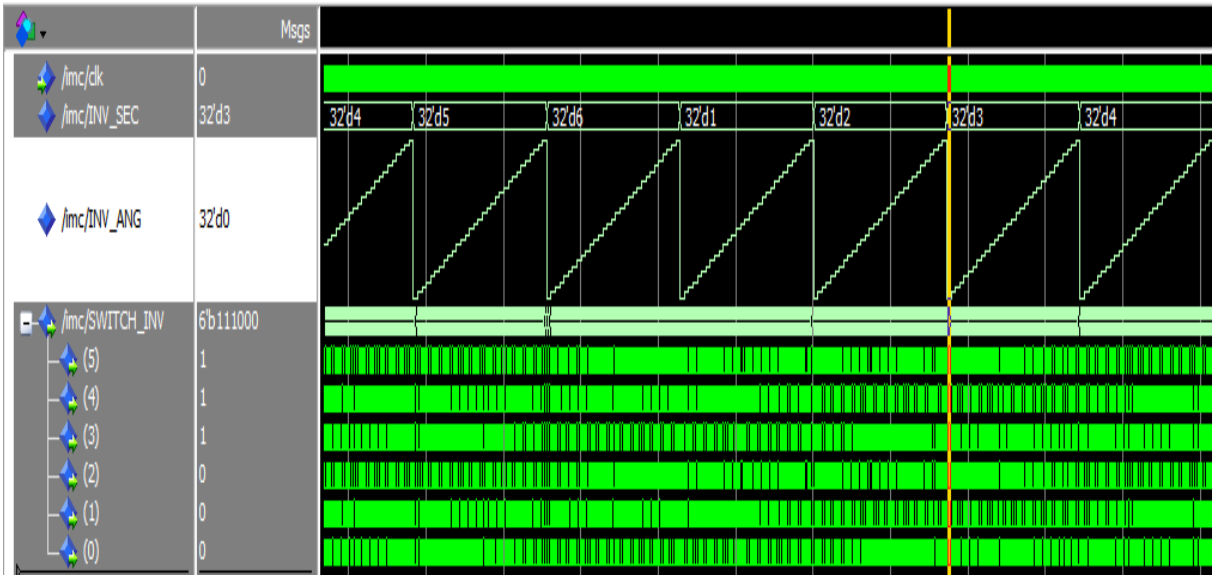

Figure 5.4: Angles, Sectors and Switches of the Inverter.

The switching time of the inverter is shown in figure 5.5.We can clearly see that at the rising edge of outt1 the switching time is TR1, and at the falling edge it takes TR2.

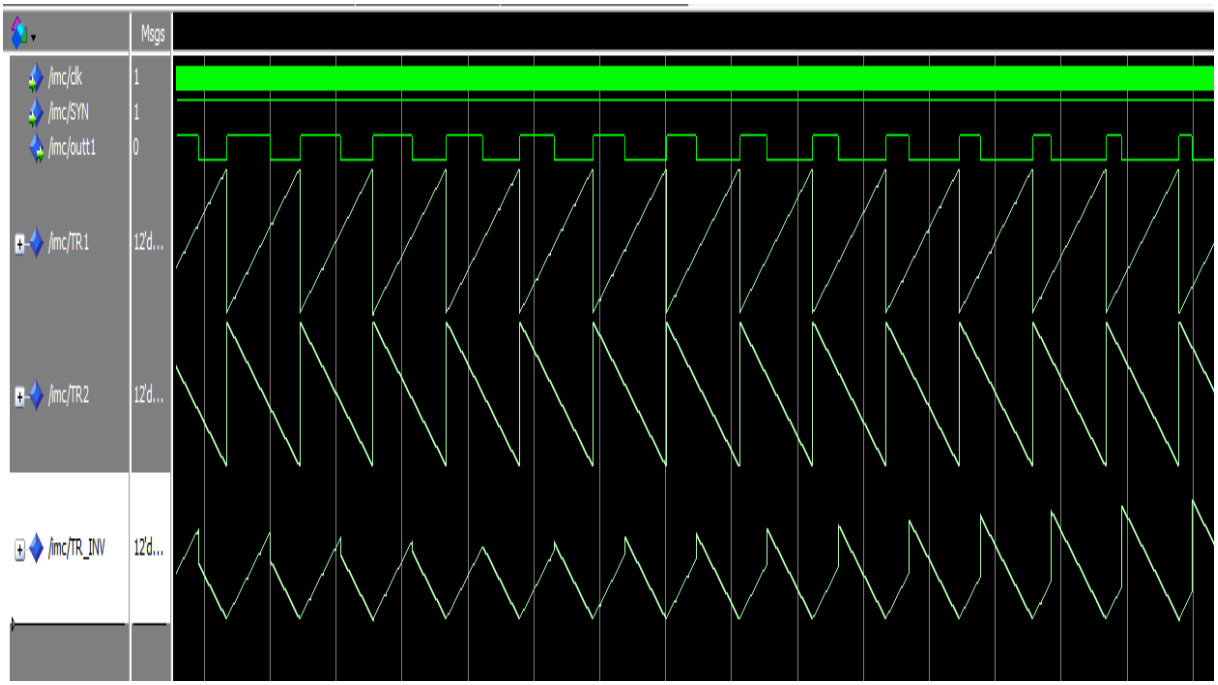

Figure 5.5: Switching Time of the Inverter.

5.4 The hardware part

5.4.1 Power supply circuit:

Four power supply circuits are needed to implement the nine gate drive circuits of the rectifier side. Transformers with turn ratio 110 V/15 V are used to step down the voltage.

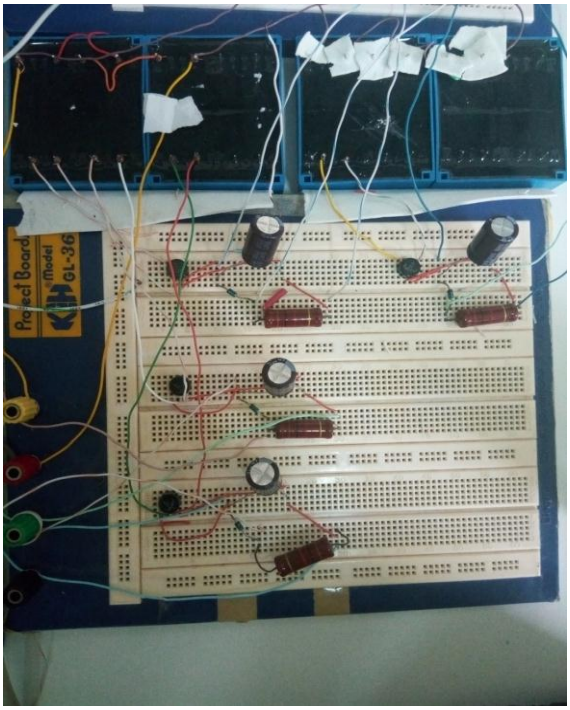

Figure 5.6: Power Supply Circuit.

Figure 5.7: Step-Down Transformer.

The voltage transmitted from the power supplies to the gates drive circuits is shown in figure 5.5.

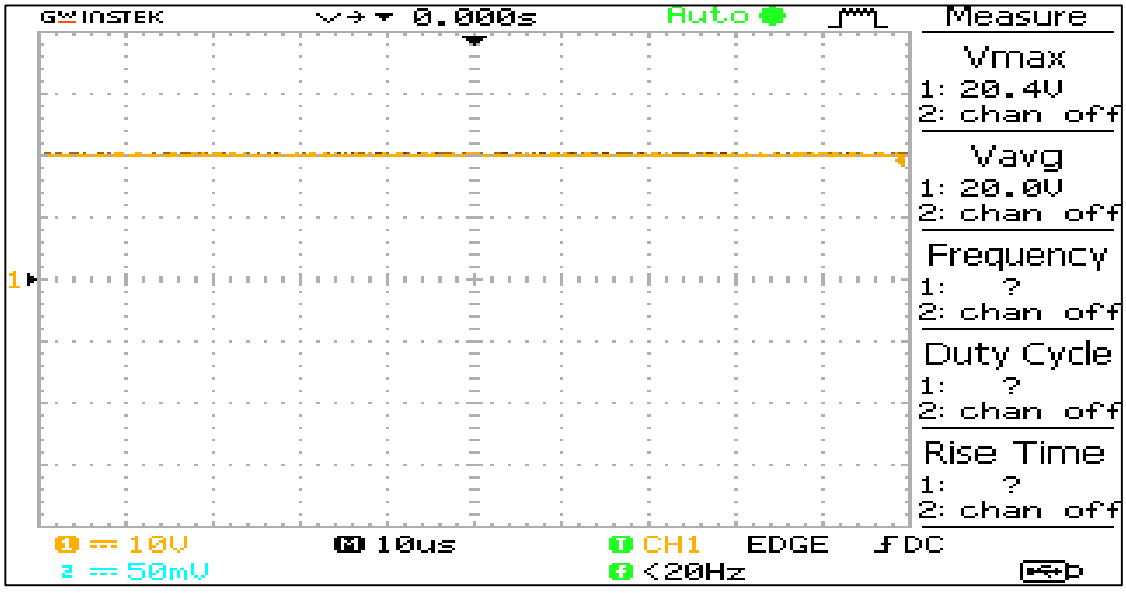

Figure 5.8: The Voltage Generated by the Power Circuit.

5.4.2 Gate drive circuits:

Nine gate drive circuits are constructed to isolate the power circuit from high power. Optocouplers HCWN3120 are used to implement the gates drive circuits.

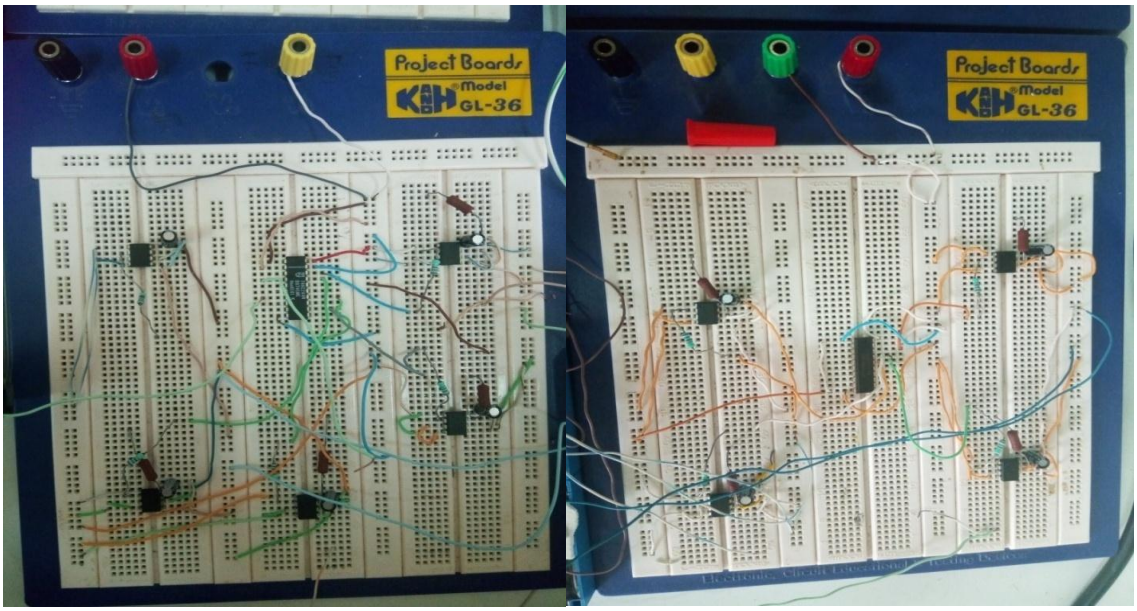

Figure 5.9: Gate Drives Circuits.

5.4.3 Power circuit:

The following figure shows the power circuit of the rectifier where three legs are implemented using 9 MOSFETs and 12 diodes.

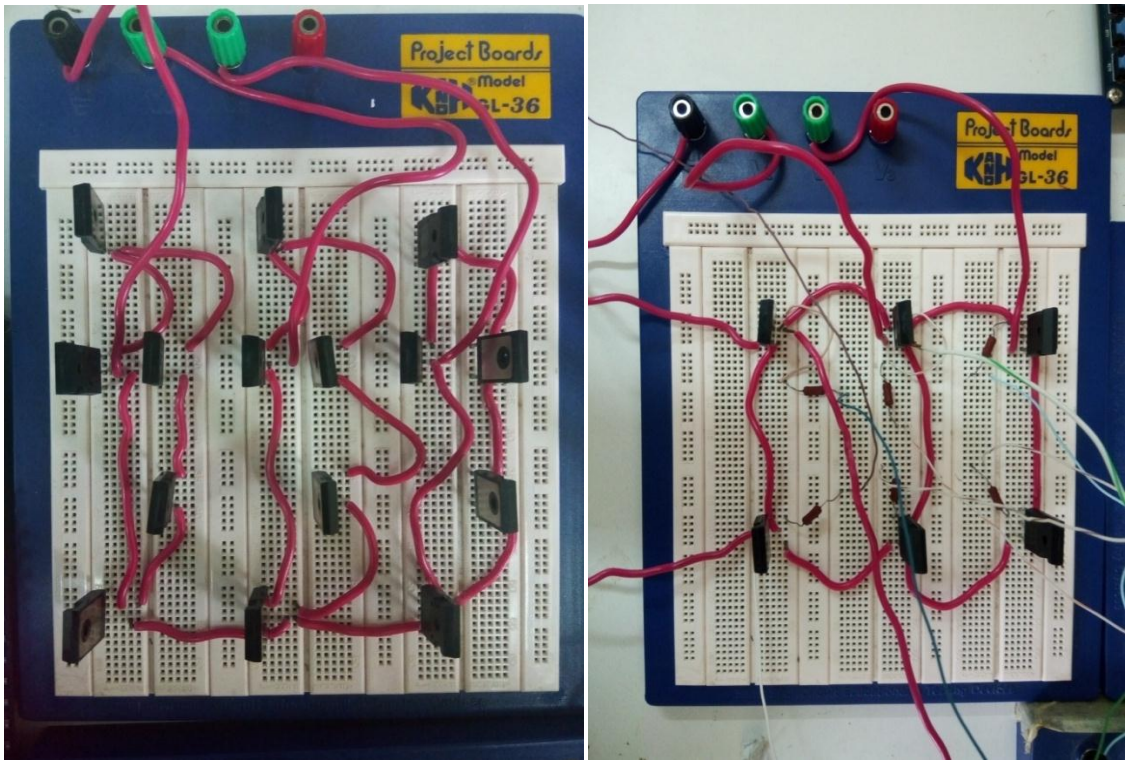

Figure 5.10: The Power Circuit: a) Rectifier Side; b) Inverter Side.

5.4.4 Synchronization circuit:

Figure 5.9 represents a circuit built using two optocouplers (LM358P, 4N37) to synchronize the phase voltage coming from the grid with the rectifier side of the power circuit.

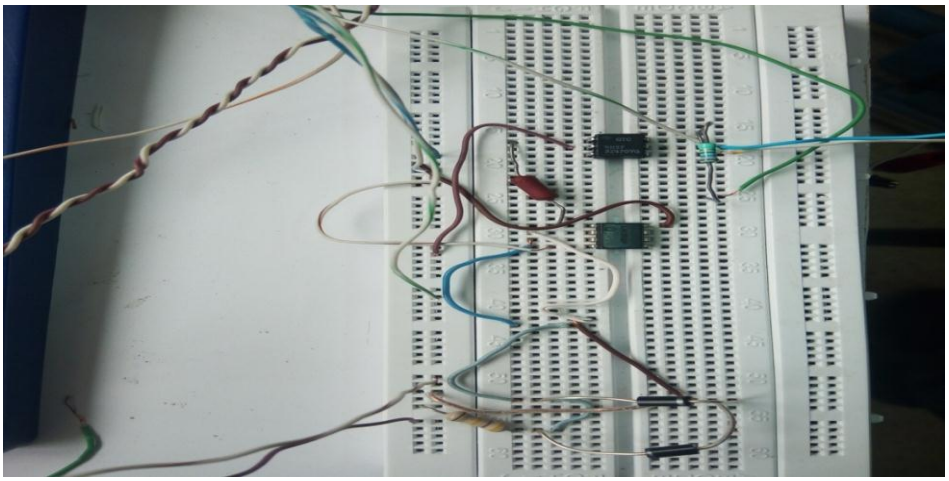

Figure 5.11: The Synchronization Circuit.

The signal used to synchronize between the grid and SMC is shown in figure 5.10. The operational sector will be chosen from the six sectors according to the rising edge of the synchronization signal, knowing that, the first sector of the rectifier starts at 30° and the one of the inverter starts at 0°.

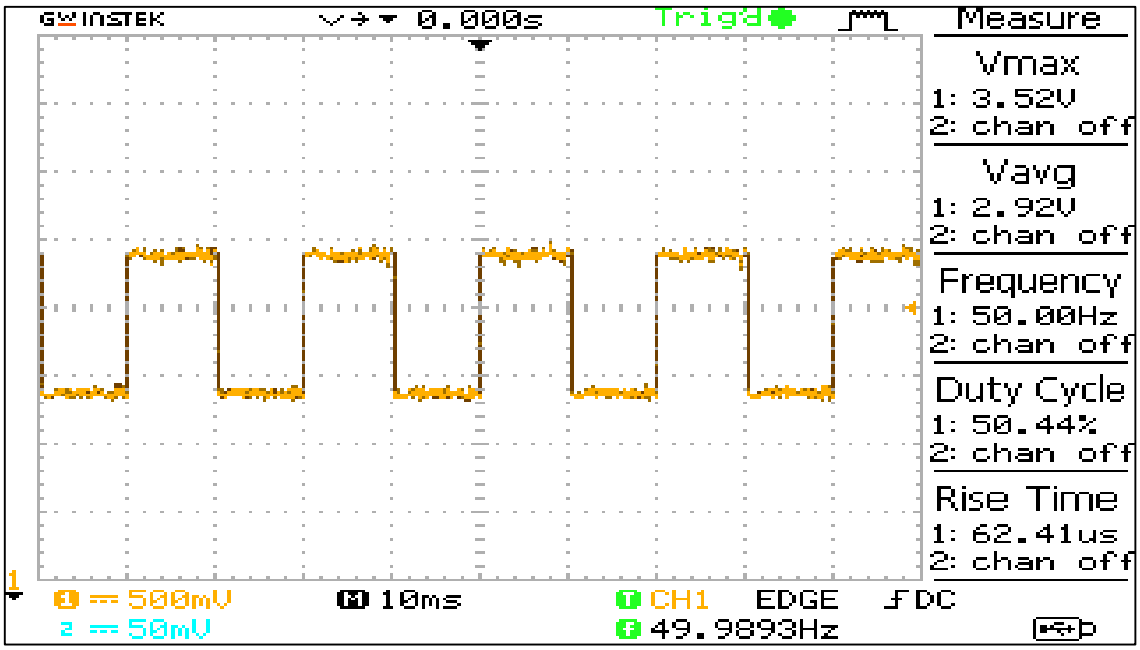

Figure 5.12: Signal Generated from the Synchronization Circuit.

5.4.5 The FPGA DE2 board:

The VHDL code is uploaded to the FPGA and then injected into the rectifier to control the commutation systems.

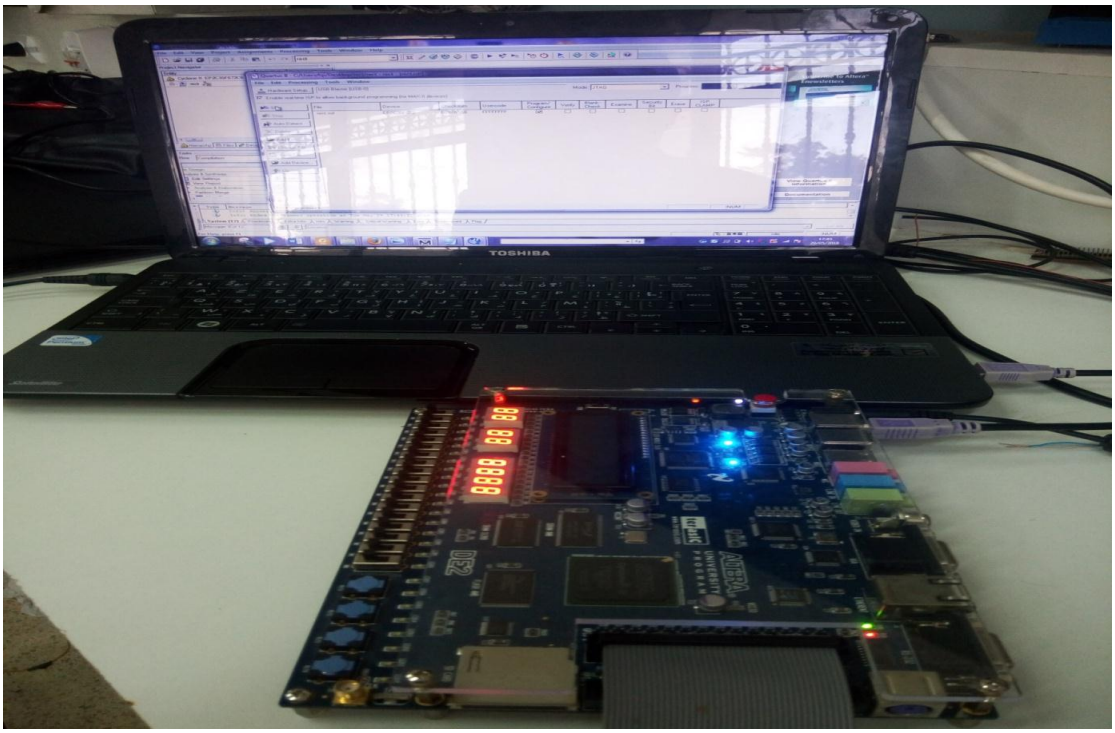

Figure 5.13: VHDL Code Uploaded into the FPGA DE2 Board.

Figure 5.14 shows the PWM of both rectifier and inverter side respectively generated from the FPGA

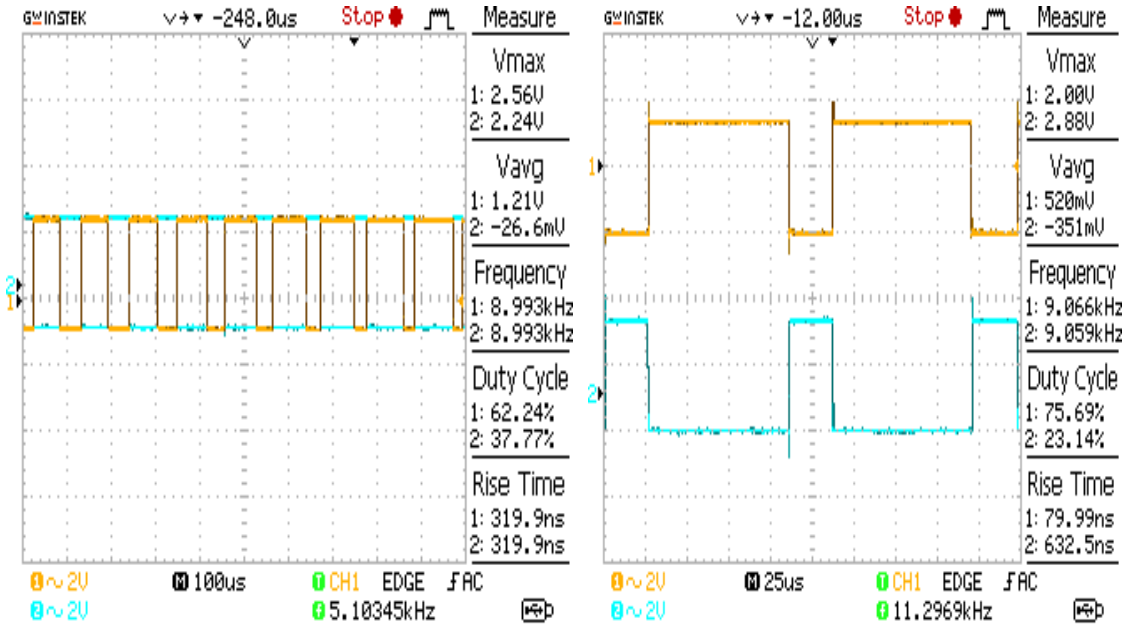

Figure 5.14: Switching Pulses of the Rectifier and Inverter Sides.

Figure 5.15 shows the dead time when the commutation occurs.

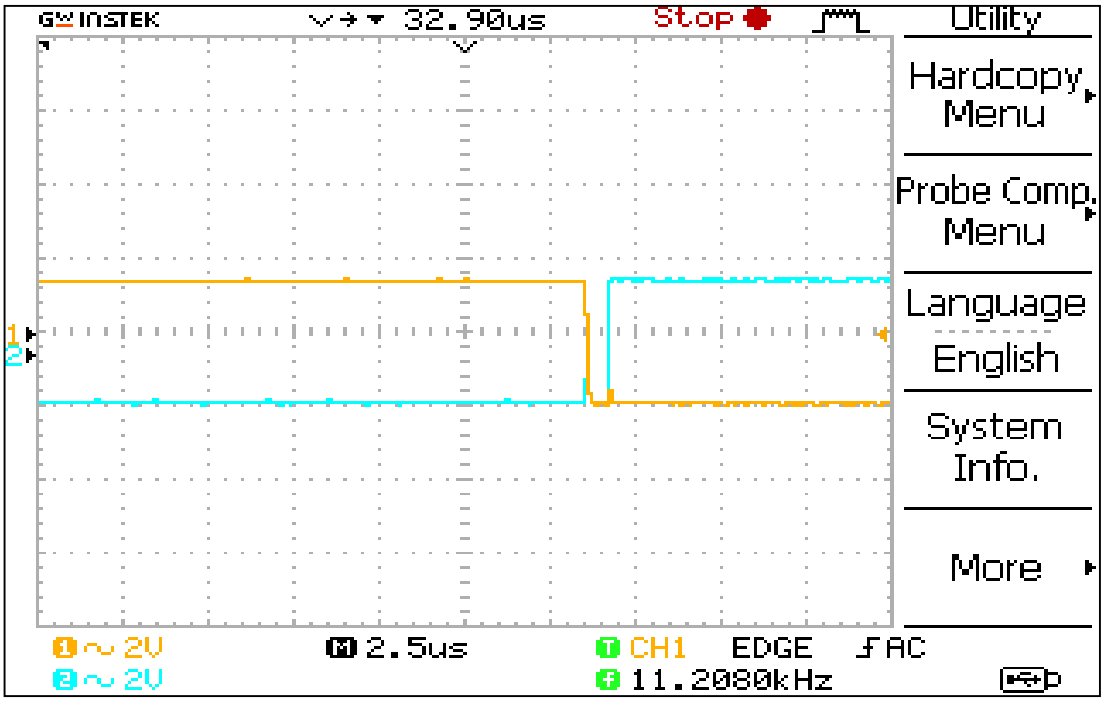

Figure 5.15: Dead Time of the Commutation.

The overall circuit implementation is shown in figure 5.12

Figure 5.16: The Overall Circuit.

5.5 Discussion

The results obtained show how the generated switching pulses are organized, the switching arrangements are independent from leg to leg and also, the inversely proportional relation between the one leg switches is shown, in other words, no interrupt between the switching pulses is encountered.

5.6 Conclusion

This work has described the general procedure of the FPGA based implementation and Control of the Sparse Matrix Converter. The different components constituting the SMC where introduced as well as the arrangement of the whole system realized in the laboratory. Switching pulses behavior and their relationship where analyzed.

Conclusion

The work presented in this thesis has made an exciting contribution to the research applications of Matrix Converters. One interesting aspect of the development of Matrix Converter driven power supplies is the power electronics employed to drive loads which operate under different conditions. The novelty introduced by the work of this thesis is to offer an alternative topology of power converter, the Matrix Converter to drive loads in different condition of operation, instead of the conventional Voltage Source Inverter (VSI) currently used in most power supply systems. the DC link and associated input filters add volume and complexity. To create the equivalent capacitance sized for the DC link using film capacitors would require a considerable amount of space compared to electrolytic capacitors. This space is usually around 30% more of that used for the electrolytic capacitors.

The area of MCs has shown continuous development in recent years in terms of new topologies of the matrix converter and the associated controlling algorithms was investigated. Theoretical background of the simulation results of the sparse indirect three-phase-to-three-phase AC-AC matrix converter topologies were presented. This thesis has presented a number of control methods that are highly investigated today, which, in principle, exhibit good performance [3], [8]. These methods have different theoretical principles and different degrees of complexity. With the results reported in this paper, space vector modulation appears as the most promising alternative due to its simplicity and flexibility to include additional aspects in the control.

The results of the simulation and experimental test proved that the converter successfully complied with its specifications. the three-phase sparse matrix converter can be used as a replacement of the conventional rectifier-inverter based converter. The advantages of the matrix converter in short are:

-Inherent four-quadrant operation

-Absence of bulky DC-link electrolyte capacitors, new control methods, and applications.

Future Work

Reduction of the number of the DC power supplies for both rectifier and inverter needed to feed the upper side constituting the SMC will be of great benefits.

References

[1] Ka´zmierkowski MP, Krishnan R, Blaabjerg F (2002) Control in power electronics: selected problems. Academic Press Series in Engineering, New York.

[2] Alberto Alesina and Marco G. B. Venturini, \Solid-state conversion: A fourier analysis approach to generalized transformer synthesis," IEEE Transactions on Circuits and Systems, vol. CAS-28, No. 4, pp. 319 { 330, April 1981}.

[3] Alberto Alesina and Marco G. B. Venturini, \Analysis and design of optimum-amplitude nine-switch direct AC-AC converters," IEEE Transactions on Power Electronics, vol. 4, Issue 1, pp. 101 { 112, January 1989}.

[4] Donald G. Holmes and Thomas A. Lipo, \Implementation of a controlled rectifier using AC-AC matrix converter theory," IEEE Transactions on Power Electron-ics, vol. 7, No. 1, pp. 240 { 250, January 1992}.

[5] Holmes DG, Lipo TA (2003) Pulse width modulation for power converters. Principle and practice. IEEE Press, New York.

[6] Kolar JW, FriedliT,KrismerF,Round SD (2008) The essence of three phaseAC/AC converter systems. In: Proceedings of power electronics and motion control conference, EPE-PEMC'08, Pozna´n, Poland, pp 27–42.

[7] Patel H, Hoft RG (1973) Generalized techniques of harmonic elimination and voltage control in thyristor inverters: Part I, Harmonic elimination. IEEE Trans Ind Electron.

[8] Patel H, Hoft RG (1974) Generalized techniques of harmonic elimination and voltage control in thyristor inverters: Part II, Voltage control techniques. IEEE Trans Ind Electron IA 1O(5).

[9] PawełSzczes´niak,University of ZielonaGóra,Three-Phase AC–AC Power Converters Based on Matrix Converter Topology, 2013.

[10] Saul Lopez Arevalo,University of Nottingham, Matrix Converter for Frequency Changing Power Supply Applications, January 2008.

[11] Thomas H. Barton, Rectifers, Cycloconverters, and AC Controllers, Oxford University Press, Oxford, United Kingdom, 1994.

[12] Bimal K. Bose, Modern Power Electronics and AC Drives, Prentice-Hall, Inc, New Jersey, USA, 2002.

[13] Alberto Alesina and Marco G. B. Venturini, \Solid-state conversion: A fourier analysis approach to generalized transformer synthesis," IEEE Transactions onCircuits and Systems, vol. CAS-28, No. 4, pp. 319 { 330, April 1981}.

[14] AlbertoAlesina and Marco G. B. Venturini, \Analysis and design of optimum-amplitude nine-switch direct AC-AC converters," IEEE Transactions on Power Electronics, vol. 4, Issue 1, pp. 101 { 112, January 1989}.

References

[15] VeeradatePiriyawong, SIRINDHORN INTERNATIONAL THAI GERMAN GRADUATE SCHOOL OF ENGINEERING Design and implementation of simple commutation method Matrix Converter.

[16] M. Venturini, "A new sine wave in, sine wave out, conversion technique eliminates reactive component", in Proc. POWERCON 7, 1980, pp. E3-1-E3-15.

[17] Huber, L. and D.Borojevic, 1995. Space vector modulated three phase to three phase matrix converter with input power factor correction. IEEE Trans. Ind. Appl.,31 : 1234-1246

[18] Patrick W. Wheeler, Jon C. Clare, Lee Empringham, Michael Bland, and Mau-

rice Apap, \Gate drive level intelligence and current sensing for matrix converter

current commutation," IEEE Transactions on Industrial Electronics, vol. 49, No.

2, pp. 382 { 389, April 2002}.

[19] M. J. Bland, P. W. Wheeler, J. C. Clare, and L. Empringham, \Comprison

of bi-directional switch components for direct AC-AC converters," 35th Annual

IEEE Power Electronics Specialists Conference, 2004, vol. 4, pp. 2905 { 2909,

2004}.

[20] Bimal K. Bose, Modern Power Electronics and AC Drives, Prentice-Hall, Inc, New Jersey, USA, 2002.

[21] Kenichi Iimori, Katsuji Shinohara, Kichiro Yamamoto, A Study of Dead-time of PWM Rectifier of Voltage- Source Inverter without DC Link Components and Its Operating Characteristics of Induction Motor, 2004

[22] Mahlein J,BraunM(2000)Amatrix converter without diode clamped over-voltage protection. In: Proceedings of international power electronics and motion control conference, IPEMC 2000, vol 2, Beijing, China, pp 817–822.

[23] Venturini M, Alesina A (1980) The generalized transformer: a new bi-directional sinusoidal waveform frequency converter with continuously adjustable input power factor. In: Proceedings of IEEE power electronics specialists conference, PESC'80, pp 242–252.

[24] G. Roy, L. Duguay, S. Manias, and G. E. April, \Asynchronous operation of cycloconverter with improved voltage gain by employing a scalar control algorithm," IEEE IAS Conference Record, 1987, pp. 889 { 898, 1987}.

[25] M. Venturini, \A new sine wave in sine wave out, conversion technique which eliminates reactive elements," Proceeding Powercon 7, vol. E3, pp. 1 { 15, 1980}.

[26] Szcze´sniak P (2009) Analysis and testing matrix-reactance frequency converters. PhD thesis (in Polish), University of Zielona Góra, Zielona Góra.

[27] P. Wood, \General theory of switching power converters," IEEE Power Electronics Specialists Conference, PESC'79, pp. 3 { 10, June 1979}.

[28] Alberto Alesina and Marco G. B. Venturini, \Analysis and design of optimum-amplitude nine-switch direct AC-AC converters," IEEE Transactions on Power Electronics, vol. 4, Issue 1, pp. 101 { 112, January 1989}.

References

[29] N. J. Mason, P. W. Wheeler, and J. C. Clare, \Space vector modulation for a 4-leg matrix converter," 36th IEEE Power Electronics Specialists Conference, 2005, pp. 31 { 38, September 2005}.

[30] Wei, L. and T.A. and Lipo, A noval Matrix Converter Topology with Simple Commutation. Record on the 26th IEEE Industrial Applications Society Annual Meetings, Chicago,, 2001. 3: p. 1749-1754.

[31] Domenico Casadei, Giovanni Sera, Angelo Tani, and Luca Zarri, \Matrix converter modulation strategies: A new general approach based on space-vector representation of the switch state," IEEE Transactions on Industrial Electronics, vol. 49, No. 2, pp. 370 { 381, April 2002}.

[32] Gebrehiwet Gebregergis_three phase matrix converter_2004.

[33] ETH Zurich Power Elecctronics Systems Laboratory ETH Zentrum/ETL H22 Physikstr.3;CH-8092 Zurich switzerland .